6 Clusters of Galaxies

Richard Bower
Department of Physics, University of Durham, Durham, UK

Abstract: This chapter focuses on galaxy clusters, tackling three aspects. Firstly, we look at clusters as laboratories, where we can study galaxy evolution and the interaction of galaxies with their environment. By measuring the properties of galaxies in clusters as a function of redshift, we can build a statistical history of galaxy formation and test this against theoretical models. Secondly, we look at the diffuse intra-cluster medium (ICM) that pervades galaxy clusters. This plasma makes accounts for the vast majority of baryons in the cluster. X-ray emission from the plasma can be used to measure the gravitational potential and to trace the thermal history of the universe. Finally, we look at clusters as probes of cosmology and their role in complementing the cosmic microwave background in constraining cosmological parameters.

1 Introduction

1.1 What Is a Cluster?

What is a cluster? Clusters are self-gravitating systems of galaxies, hot gas, and dark matter. By convention, they have typical masses of 10^{14}–$10^{15}\,M_\odot$ and contain 100s–1,000s of galaxies. We distinguish clusters by their mass. They are the most massive collapsed objects in the present-day universe. Clusters are rare, and even the least massive have a space density less than $\sim 10^{-5}\,\mathrm{Mpc}^{-3}$. The most massive examples have a space density of $\sim 10^{-8}\,\mathrm{Mpc}^{-3}$ in the local universe. The space density declines rapidly to higher redshifts. Our nearest rich cluster, the Coma cluster, is a good example of fairly typical galaxy cluster (see ❯ *Fig. 6-1*). Its close proximity makes it possible to study the galaxy properties in great detail.

We often refer to lower mass (and more common) systems with masses in the range $10^{14}\,M_\odot > M_{\mathrm{tot}} > 10^{13}\,M_\odot$ as galaxy groups. There is no strict definition of the mass limits, however, and some authors would include the systems containing two bright galaxies (e.g., the Milky Way and Andromeda) as "groups." Many papers also refer to "field" galaxies. Such galaxies are really average galaxies drawn from random locations in the universe. Consequently, some field galaxies might well lie in groups, while clusters are too rare to be represented. It is perhaps better to refer to "isolated" galaxies if we want to contrast the properties of galaxies inside and outside groups.

Our modern understanding is that clusters form as the result of gravitational instability. They are the result of small density fluctuations in the post-inflation universe. The gravitational instability creates a whole spectrum of virialized (i.e., stable) dark matter haloes. As the universe evolves, the characteristic halo mass moves to larger and larger scales. Clusters are the most massive of these haloes and exponentially rare in the present-day universe. They will become increasingly common in the future, until the acceleration driven by dark energy eventually halts development of cosmic structure.

1.2 Historical Perspective

It is helpful to begin with a brief review of the long history of galaxy cluster studies. Almost as soon as the first astronomical telescopes were developed, clusters were identified as striking concentrations of galaxies on the sky. The discovery predated the realization that the "spiral

■ Fig. 6-1

With a mass of $2 \times 10^{15}\, M_\odot$, the Coma cluster is our nearest large cluster. It lies at a distance of 100 Mpc. The image shows the central regions of the cluster and is annotated with some of the brighter galaxies catalogued by early astronomers. The cluster is often used as the archetypal cluster. Nevertheless, the cluster may have resulted from a recent merger of two smaller systems resulting in the two dominant galaxies, NGC 4884 and NGC 4874 (Image credit: NASA/DXS)

nebulae" were outside our own galaxies. A clear division in galaxy properties was already evident in these observations, and it was immediately evident that most galaxies in clusters were amorphous systems, devoid of spiral arms. This density–morphology relation has been the motivation of a great deal of "ecological" research over past decades. The central questions have morphed into a consideration of the star formation histories of galaxies, but the issues are still the same.

The development of spectrographs allowed the redshifts (and hence relative velocities) of galaxies to be measured. This lead to an apparent contradiction: if clusters were bound, the mass associated with each of the galaxies must greatly exceed the visible stellar mass. Zwicky had discovered the existence of dark matter. Of course, these observations do not make it clear that the dark matter is non-baryonic. The discovery of the hot gas in clusters had to wait until the development of X-ray balloon observations. The discovery of bright X-ray emission was a great surprise, but it was quickly realized that the mass of hot gas trapped by the gravitational potential greatly exceeded that in visible stars.
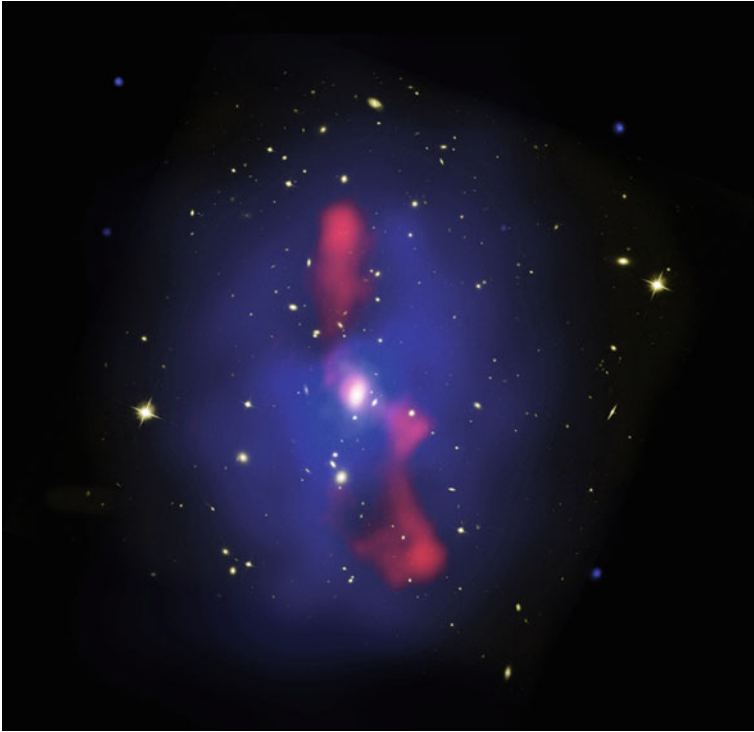
◨ Fig. 6-2

An example of the spectacular interaction between a radio galaxy and the surrounding cluster. This image shows the cluster MS0735.6 + 7421 (McNamara et al. 2005) and superposes the optical (*yellow*), X-ray (*blue*), and radio (emission). The jet of radio emission from the central galaxy has swept aside the intra-cluster medium creating a cavity in the X-ray-emitting plasma. Such events are hugely energetic and are thought to balance the radiative cooling of the intra-cluster medium (Image credit: NASA/CXC/SAO)

The discovery of hot gas, however, leads to a new puzzle. The luminosity implied a high cooling rate. Surely, this cooling gas must go somewhere, and surely, it must lead to the formation of stars. The "cooling flow" paradox was born. A paradox because the cooling rates seemed incompatible with the red colors and low rates of star formation in cluster galaxies. Some authors suggested that the gas might form rocks or invisible low-mass stars, but resolution would have to wait for the vastly improved image quality and spectroscopic energy resolution of X-ray satellites.

A key piece of the puzzle is the frequent association of "radio galaxies" with clusters. Such galaxies have strong radio emission, frequently in the form of jets generated by accretion onto a central black hole. An example is shown in ❯ *Fig. 6-2*. Thus, the story of galaxy clusters links the collapse of dark matter on cosmological (100 Mpc or 10^{24} m) scales to the accretion physics on the scale of the black hole horizon (scales of 10^{11} m).

More recently, gravitational lensing has provided overwhelming evidence of the existence of dark matter. Although the bending of light was an early prediction of general relativity, it was

◻ Fig. 6-3
The galaxy cluster A2218. The image highlights the spectacular gravitational lensing created by gravitational potential of this cluster. The arc-like features in this image are the distorted images of background galaxies. The source is strongly magnified making, it possible to exploit the cluster as a gravitational telescope. In addition to this strong lensing effect, the cluster weakly distorts the shapes of background objects across the entire field. Inverting this distortion provides a means of directly measuring the cluster's mass (Image credit: NASA/HST)

not widely appreciated that clusters were so massive that they would easily bend light from background objects into spectacular giant arcs. Initial explanations suggested that these were galaxies being ripped apart by the tidal forces of the cluster, but spectroscopy clearly showed them to be objects at much greater distance than the cluster. Spectacular arcs have now been observed from young galaxies at $z = 5$ and greater (❯ *Fig. 6-3*).

The discovery of gravitational lensing has ushered in a new era of cluster studies, where the mass content and concentration of galaxy clusters can be determined without reference to the galaxy content or the X-ray hot gas. This has made it possible to directly calibrate the masses of clusters and thus to use them as probes of galaxy evolution. More startlingly, the clusters can also become telescopes, gravity creating the first lens of a cosmic telescope that provides an unprecedented views of the first galaxies to form in the universe.

1.3   Overview

In this chapter, I will take the reader on a guided tour of forefront studies of galaxy clusters. This will begin with a close look at the optical properties of clusters and the galaxies they contain. I will examine the special morphologies and star formation histories of cluster galaxies compared to those in more isolated environments. The aim is to understand how the differences between these galaxies are established. This has led to better understanding of Galaxy Ecology – the ways in which galaxies interact with their surroundings – and to improved understanding of the suppression of star formation in the universe in general. An important topic at the present is to compare the properties of galaxies in presented day clusters with those of clusters at higher redshifts. The higher redshift clusters are seen at earlier times and are (in a statistical sense) the progenitors of toady's most massive systems. This is a fertile test-bed for theories of galaxy formation and evolution.

Although clusters are often thought of as collections of galaxies, galaxies are far from the dominant baryonic component. A far greater fraction of the system's baryons are associated with a diffuse hot plasma that is confined by the gravitational pull of the system's dark matter. The plasma is a strong X-ray emitter, and the spectrum can be analyzed to reveal the plasma density and temperature. This allows the cluster to be used as cosmic calorimeter reflecting the thermal history of its formation. I will discuss the major puzzle of this plasma – the "cooling flow paradox." Although the plasma has a short cooling time, the measured star formation rates of cluster galaxies are much smaller than this would seem to imply. The resolution to this paradox seems to be intimately connected to the frequent presence of radio galaxies in cluster of galaxies, an observation that has now been incorporated into theoretical models of galaxy formation with profound consequences.

In the final section, I will look at clusters of galaxies from a theoretical perspective, focusing on the evidence for their dark matter content and on their role in setting cosmological parameters. I will also set the formation of clusters of galaxies in the context of the growth of the large-scale structure of the cosmos.

2   The Optical Properties of Clusters

2.1   The Density–Morphology Relation

Galaxies contain two main components – a flattened stellar disk that is supported by the coherent rotation of stars and an ellipsoidal bulge that is supported the random and roughly isotropic motion of its stars. Hubble developed a system for classifying galaxies on the basis of (1) the relative strength of the disk and bulge components and (2) the presence and strength of spiral arms. Galaxies with a dominant bulge component and weak spiral arms are referred to as "early type" while the galaxies with a strong disk and clear spiral arms are "late types." The designation is not intended to indicate a morphological sequence. The late or spiral galaxies are then subclassified according to the presence of a central bar as well as the strength of the bulge/spiral arms. An important class of galaxies is the lenticular or S0 galaxies. These have a clear disk component (as well as a strong bulge) but weak or absent spiral arms. Elliptical galaxies have significantly weaker (or undetectable) disks. From the view point of clusters, the key distinction is between the early and late types and between the elliptical and S0 galaxies.

Dressler (1980) applied the classification scheme to clusters of galaxies. This was a heroic work obtaining clear photographic plates and laboriously classifying the galaxies in the clusters. Although it had been clear to even the first observers (such as Herschel and Wolfe) that early types were clustered into the densest regions, Dressler's measurements made it possible to quantify this trend. The results showed a universal relationship between the local density and galaxy type, and Dressler used this to argue that there was a causal connection between galaxy morphology and clustering. More recent results have been used to show that the trends extend to lower density environments such as galaxy groups and that the development of the relation can be traced back to high redshift.

The origin of galaxy morphology is often phrased in terms of "nature vs. nurture." In other words, is the morphology of galaxies a result of the initial conditions of galaxy formation, or as the result of the later evolution of the galaxy? Were the galaxies formed differently and then captured into the cluster, or were they modified by the cluster? Current theories suggest that both play a role. The galaxies in clusters (and groups) tend to be more massive than galaxies in lower density environments. This describes a large part of the trend since more massive galaxies are very often elliptical. But a trend with environment is still evident at a fixed stellar mass, and this is ascribed to various physical processes that tend to suppress star formation in cluster galaxies (converting spirals to S0 types as the disk fades and the arms dissolve) and to randomize the coherent disk motion to form a bulge (converting S0 to elliptical types). Ram-pressure stripping of disk and halo gas is thought to drive the spiral to S0 transformation, while the S0 to E transformation is most likely driven by galaxy collisions/mergers and harassment (the cumulative effect of weak encounters). Theoretical models for galaxy evolution make an important distinction between the galaxy at the center of the system and the satellite galaxies that orbit around it. We should expect the satellites to be subject to the transformation processes, while the central galaxy may continue to accrete further gas from its surroundings. I will describe the transformation processes in more detail below. The timescales for the two transitions need not be the same.

At higher redshift, the trends evolve, with higher redshift clusters containing a higher proportion of later-type galaxies. A particularly contentious issue has been the rapid buildup of the S0 content of clusters. The controversy has largely arisen due to the difficulty of clearly distinguishing the E and S0 types and in allowing for the biases in clusters/galaxy selection due to the redshifting of the observed bands.

A major effort has therefore been made to establish a morphological classification scheme that can be determined by computers rather than the human eye. Machine-based schemes use the light profile or the concentration and asymmetry (Simard et al. 2002). Some success has been obtained in describing the broad-brush evolution of the galaxy population as a whole, but the differences in the morphologies of cluster galaxies are rather more subtle. Indeed, the issue of mapping machine-based classifications onto Hubble scheme is difficult because the original classification scheme relies on more than one property.

A new development is the "Galaxy Zoo" (Lintott et al. 2008; Bamford et al. 2009): using a popular web site, "citizen-scientists" are invited to classify galaxy images (currently from the Sloan Digital Sky Survey). Although each individual classifier may have a large uncertainty in classifying one object, each galaxy is classified by hundreds of people so that the trends can be carefully examined with statistical tools. Recent results present a reassuring confirmation of the trends identified by Dressler but emphasize that galaxy mass has at least as important a role as galaxy environment.
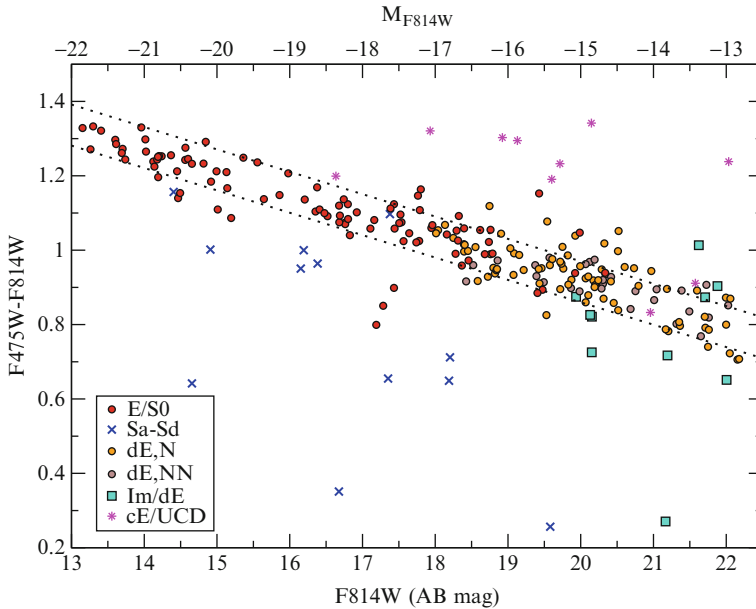
2.2 The Color–Magnitude Relation

The lack of a clear physical interpretation of galaxy morphology has led many authors to prefer classification schemes based on galaxies, stellar populations and star formation histories. In outline, spiral galaxies have significant contributions from young, relatively hot stars (this makes the spiral arms stand out in imaging data), while elliptical and S0 galaxies are dominated by older stars similar to the sun. Color (or certain spectral absorption lines) may therefore be used to create a classification scheme that is clearly related to underlying physical properties of the galaxies. The universe encourages us to use this scheme since galaxies fall onto two largely separated sequences of passive galaxies (with red colors and little ongoing star-formation) and star-forming galaxies (with blue colors and specific star formation rates around $0.1\,\mathrm{Gyr}^{-1}$, such galaxies will double their stellar mass in 10 Gyr which suggests that their average star formation rate has changed little over the history of the universe).

Galaxy color has the advantage that it is relatively "cheap" (in terms of telescope exposure time) to measure and that the average color of the whole galaxy can be determined (making it simple to compare galaxies of different angular size). Colors have the drawback that they are affected by both the age of the stellar population and its star formation history. This degeneracy can make it hard to interpret results uniquely, although the situation is improved by using several colors spanning along wavelength base line, preferably including data from the near-infrared. It is also difficult to determine instantaneous star formation rates from optical/near-IR data: so, additional data in the ultraviolet or mid-infrared is required. Spectra of galaxies contain more information than galaxy colors, allowing instantaneous star formation rates to be determined from strong nebular emission lines (such as $H\alpha$) and allowing the age-metalicity degeneracy to be broken using carefully selected stellar absorption features. This is an extensive topic. Nevertheless, a great deal can be learned from a look at the broadband optical colors of cluster galaxies, particularly if the galaxy redshift is known (or can be accurately estimated using multiple photometric bands).

The standard approach is to plot galaxy color as a function of luminosity. In clusters, a clear sequence of red galaxies stands out. An example (for the Coma cluster) is shown in ❯ *Fig. 6-4*. All the galaxies in this plot are confirmed to have redshifts matching that of the cluster. The close proximity of the cluster makes it possible to measure accurate colors for even very faint galaxies and to show that the sequence extends over a range of 10,000 in stellar mass.

The existence of this relation places strong constraints on the formation history of cluster galaxies, as well as making clusters stand out in imaging of random fields. The relation is so red because the majority of the cluster galaxies have few young stars: the bulk of the stars in these systems must have formed many Gyr in the past. If we focus on the cores of galaxy clusters, the very small proportion of cluster galaxies that deviate to the blue side of this sequence implies that few star-forming galaxies are present and the fraction of blue galaxies can be used to establish an analog of the morphology–density relation. The slope of the red sequence can be understood in terms of a stellar mass – metalicity and stellar mass – age relationships. These relationships appear to be universal from cluster to cluster, implying a great deal of similarity in cluster formation history.

The cluster can be contrasted with a random field where the galaxy colors are much more smoothly distributed in the color plane. Although a red-sequence is also evident in the random field, it is occupied by a far smaller fraction of galaxies (recall that the random field will include galaxy groups in the sample). However, the spread in the red shifts of the field systems means

The color-magnitude relation in the Coma cluster. The points show the strong correlation between the brightness of cluster galaxies and their color. The points are labeled by morphology. The relation obeyed by the early-type (E/S0 and dwarf E) galaxies is extremely tight with a scatter of less than 0.06 mag. In these spectacular observations, the relation is seen to hold over 10 mag in galaxy luminosity (a factor of 10,000 in galaxy mass) (Image credit: Hammer et al. 2010)

that the sequence (and the corresponding bluer sequence of star-forming galaxies) is smeared out. This makes it possible to effectively select clusters of galaxies using optical techniques, capitalizing on the enhanced the contrast of the cluster against the projected background of the field galaxies (Gladders and Yee 2000).

2.3 Spectroscopic Properties of Cluster Galaxies

The spectra of galaxies are, of course, essential for confirming a galaxy's membership of a cluster, but they also contain a great deal of information about the current star formation rate of galaxies, their past star formation histories, and their metal abundance.

- *Star formation rate diagnostics.* Ongoing star formation rates of galaxies can be estimated from the emission lines in the spectrum. The technique measures the total ionizing flux produced by massive stars, since this is remitted as line radiation when the interstellar gas recombines. Because hydrogen is so abundant (and has a low-ionization potential), it is particularly strong. One of the best star formation tracers is thus the Hα emission line at 6,563 Å (Kennicutt 1998; Brinchmann et al. 2004). Conversion of a line luminosity to a star formation rate is, however, complicated by the presence of dust that may scatter or absorb line photons before they leave the galaxy. It is possible to correct for this using the

relative strength of Hα and Hβ. Other elements, notably oxygen, also produce strong lines, but interpretation of these lines as star formation indicators is dependent on the system's metal abundance (as well as dust), so they must be carefully calibrated. It is also possible to estimate star formation rates on the basis of the mid-IR (e.g., 24 μ) flux. This uses the flux of UV radiation that is reprocessed by dust. In this way, it is possible to determine star formation rates even in galaxies that show no detectable emission. With all these methods, care needs to be taken that the source of flux is star formation rather than accretion on to a black hole (an AGN).

- *Star formation history diagnostics*. Absorption lines in the spectrum can be used to study the star formation history of a galaxy. This is usually parameterized as the luminosity weighted age of the stellar population. The technique relies on the different surface gravity and metallicity sensitivity of various Balmer and metal lines (Worthey 1994). Strong higher-order Balmer lines are indicative of a young stellar population. For example, an Hδ equivalent width of greater than 3 Å can only be explained by the presence of a substantial population of A-class stars. This indicates a luminosity weighted stellar age of around 1 Gyr.

- *Metalicity indicators*. The metal abundance of the stellar population can be determined from diagnostic lines in a similar way. However, the differences between lines as a function of metallicity are relatively subtle and careful modeling is required. In particular, galaxies in clusters often show an enhancement in the abundance of α process elements (such as Mg) relative to that in the solar spectrum. This provides an additional measure of the star formation history of the galaxy suggesting a relatively rapid enrichment, primarily by type II supernovae.

These techniques allow the galaxy population to be described in more detail. Current results confirm that the most massive early-type galaxies are old (age ~10 Gyr) and metal rich. There is a consistent tendency for lower luminosity galaxies to be both less metal rich and to be younger than the more massive galaxies. This may agree well with the results from the observed evolution of galaxy color–magnitude diagrams. In addition, the lower mass galaxies show less enrichment of α process elements, suggesting that they have a more extended star formation history as well as being younger (Nelan et al. 2005).

2.4 The Fundamental Plane of Early-Type Galaxies

The spectra of galaxies also allow the velocity dispersion or rotation speed of the stellar system to be determined. Combining this with the stellar radius of the system yields the dynamical mass of the galaxy. In clusters, this is most often applied to the elliptical and bulge-dominated S0 population. Since the velocity dispersion profile is approximately flat, the mass can be estimated by the simple application of the virial theorem. If we further assume that the mass is dominated by the stellar population (or at least proportional to the luminosity) and that the shape of the system is homologous, this predicts a tight correlation between the system radius, velocity dispersion, and mass:

$$R_e \propto \frac{M_e}{\sigma^2} \qquad \text{or} \qquad R_e \propto \sigma^2 I_e^{-1} \qquad \qquad (6.1)$$

where R_e is the effective radius of the galaxy, M_e the mass within R_e, σ the central velocity dispersion, and I_e the surface brightness at R_e. Such a tight correlation is indeed observed,

although the coefficients of the observed relation differ slightly (Jorgensen et al. 1996):

$$R_e \propto \sigma^{1.2} I_e^{-0.8} \tag{6.2}$$

The difference between the two appears to arise from variations in the mass-to-light ratio of the stellar population and a degree of nonhomology. Such variations are not surprising since the stellar populations are known to vary with total system mass. Indeed, many galaxy properties correlate more tightly with velocity dispersion than with system mass.

By choosing suitable combinations of the surface brightness and the velocity dispersion, the fundamental plane may be viewed edge on. The resulting tight correlation with luminosity may be used as a powerful distance indicator and also as a strong constraint on the mass-to-light ratio evolution of cluster galaxies (Holden et al. 2005).

2.5 Galaxy Ecology

Galaxy ecology is the study of how galaxies interact with their environment. Clusters make a good laboratory (Gunn and Gott 1972). There are lots of galaxies in one place, at one red-shift. The drawback is that cluster galaxies represent only a small fraction of the total galaxy population. Galaxy groups contain a much larger fraction of the population, and galaxy trans-formations, also more likely there. The subject is opening up due to large redshift surveys which identify large samples of group galaxies, but at high redshift, these surveys are still limited to relatively bright galaxies.

Although the trends of morphology and color with environment density are well estab-lished, the theoretical underpinnings of the relationships are only now becoming clear. There are essentially four key processes that transform galaxy properties: galaxy collisions, dynamical friction, the ram pressure of the intra-cluster medium, and "strangulation." However, the prop-erties of galaxies in clusters are not simply the result of galaxy transformation. Cluster galaxies are generally brighter than spirals, so the comparison needs care to ensure that galaxies are being compared on a like-for-like basis. Samples must match in stellar masses, not luminosi-ties, and the comparison must allow for tidal stripping and fading of the disk. Finally, it should be remembered that the progenitors of cluster galaxies are not the spiral galaxies we observe today, but the field galaxy population at $z \sim 1$.

2.5.1 Galaxy Collisions

Consider what happens when one galaxy passes another. The stars feel a perturbation in their gravitational force. A rapid fluctuation removes energy from the (ordered) motion of the galaxy and puts it into random motions of the stars. If the encounter is sufficiently rapid, we can use impulsive approximation. The energy transferred from the orbital motion of the galaxies to the internal motion of the stars is then

$$\Delta E \sim \frac{G^2 M_2^2}{V_p^2 R_p^2} M_1 \left(\frac{r_1}{R_p} \right)^2 \tag{6.3}$$

where M_1 and M_2 are the masses of the perturbed and perturbing galaxies, respectively, r_1 is the size of the perturbed galaxy, their relative velocity is V_p, and their closest approach distance is R_p (Richstone 1975; Covington et al. 2008).

The effect is (1) to puff up the galaxy's stellar disk. If the energy transfer is extreme, the heating destroys the disk. S0 disks are indeed thicker than those of spiral galaxies. (2) Remove orbital angular momentum. If enough is removed, the two galaxies become bound, and as they encounter each other again, more energy is lost and they spiral together eventually merging to form an (elliptical) remnant. If the galaxy masses are comparable, the remnant will be dominated by the bulge. The remnant's shape is dominated by velocity dispersion (which need not be isotropic). If the masses are unequal, a significant disk may survive.

However, these processes are more effective if the encounter speed is comparable to the motion of the stars. If it is too rapid, the energy exchange is minimal. As a result, clusters with high-velocity dispersions are not likely to be strongly influenced by collisions. "Harassment," the cumulative effect on multiple, weak encounters, may be important however (Moore et al. 1996).

2.5.2 Dynamical Friction

As a galaxy travels through the dark matter halo of the cluster, it experiences a drag force. This results because the dark matter is focused towards the galaxy as it orbits and generates a wake behind the galaxy. The slight mass excess exerts a retarding force on the galaxy's motion.

Over time, this saps the orbital energy of the galaxy. The timescale for the galaxy to sink to the center is given by

$$t_{\text{sink}} = \frac{r^2 V_c}{Gm} \frac{1}{\mathcal{F} \ln \Lambda} \tag{6.4}$$

where V_c is the circular velocity of the halo and r the initial radius of the satellite of mass m. $\mathcal{F}$ and $\ln \Lambda$ are dimensionless constants relating to the velocity anisotropy of the dark matter particles in the halo and the relative range of encounter scales (Chandrasekhar 1943). The satellite's dark matter halo also looses mass as it spirals in, tending to increase the dynamical friction timescale. These uncertainties can be calibrated by numerical simulations (Boylan-Kolchin et al. 2008).

Dynamical friction leads to galaxies spiraling into the center of the cluster. Indeed, the central galaxies of clusters have unusual properties, not seeming to fitting extrapolation of the normal luminosity function and reflecting a flattening of the galaxy mass-metalicity relation. When clusters merge, dynamical friction will cause the central galaxy of each system to merge together. This is a likely explanation of clusters, like the Coma cluster, that contain two (or more) dominant galaxies.

2.5.3 Ram-Pressure Stripping

Cluster galaxies are moving through the diffuse intra-cluster medium (ICM) and are subject to hydrodynamic forces. In particular, if the galaxy contains a disk of cold gas, it must force the ICM aside for the galaxy to pass through. If the gravitational force holding the gas in the plane of the galaxy is too weak, the gas will be stripped. This condition can be written as

$$\rho_{\text{ICM}} V^2 > 2\pi G \Sigma_*(r) \Sigma_g(r) \tag{6.5}$$

where ρ_{ICM} is the density of the diffuse external gas V in the orbital velocity of the galaxy, $\Sigma_*(r)$ is the stellar surface density of the galaxies disk at radius r, and Σ_g the surface density of gas at this radius. If the condition is satisfied, gas will be stripped from this radius. If the
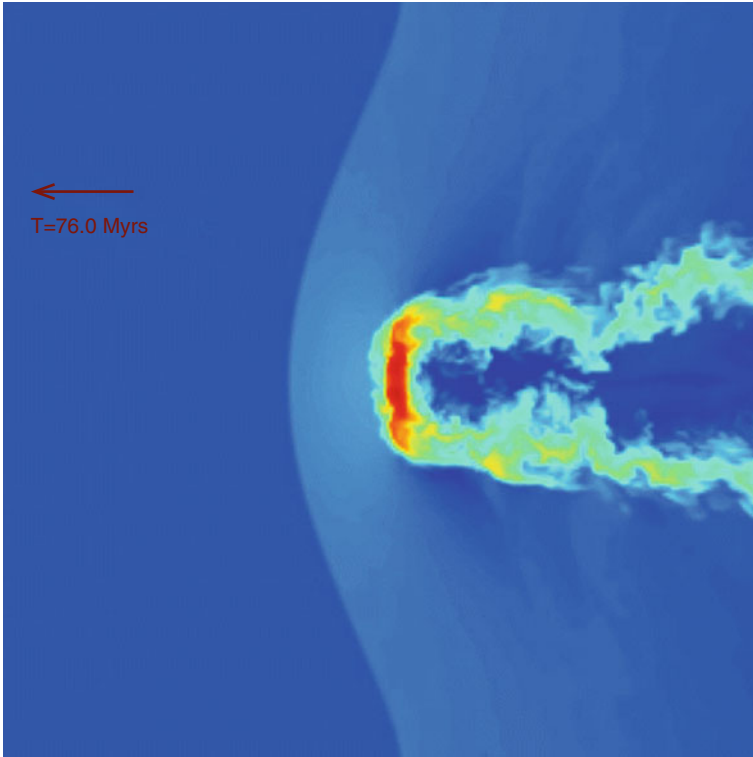
■ Fig. 6-5
A simulation of the effect of ram-pressure stripping on a spiral galaxy. As the galaxy passes through the intra-cluster medium, the ram pressure sweeps material out of its disk leaving a trail of ionized material behind it. Such trails have been observed behind spiral galaxies in clusters (Image credit: Quilis et al. 2001)

galaxy is moving sufficiently fast, all the gas in the galaxy will be removed. At lower velocity, only material in the outer parts is removed (Gunn and Gott 1972). The results of these simple analytic arguments can be verified with numerical simulations (❯ *Fig. 6-5*). These show that the formulae are broadly correct (Quilis et al. 2001), but highlight a number of potential issues such as the compression of the interstellar medium during the stripping process.

The ram-pressure stripping mechanism presents a plausible explanation of the absence of conventional spiral galaxies in clusters. Indeed, some examples of galaxies in the process of being stripped have been clearly identified through high-resolution ultraviolet imaging of galaxies in nearby clusters. However, the stripping process is only likely to be strong if the motion of the galaxy is rapid and the ICM is sufficiently dense. Since lower mass systems, such as galaxy groups, contain a much lower density plasma, this is not likely to explain the relative abundance of the early-type galaxies in groups. Yet, observations of galaxy groups show that the passive galaxy sequence and many of the characteristic properties of cluster galaxies are already established in lower mass groups. It seems that this mechanism cannot be the dominant driver of galaxy ecology.

2.5.4 Strangulation

This is a theorist's mechanism, and not directly observed. Galaxy formation models suggest that galaxies continually recycle gas between their disk and halo (White and Frenk 1991). Feedback from supernovae ejects the gas from the disk regulating the star formation rate of the galaxy. Without this process, galaxy formation is far too efficient to match the very-low-observed stellar mass fraction of the universe. (Clusters are a good census: only 10% of the cluster baryons are locked into stars.)

In cluster galaxies, this cycle is easily interrupted by ram-pressure stripping of the loosely attached material in the halo of the galaxy. This is a distinct process from the stripping of the tightly bound material in the galaxy disk. However, the process can be described by the same formula, but need to reassess the coefficient because of the relative distributions of mass and gas. Essentially, the same formula applies as for the ram-pressure stripping of disk gas but with a new coefficient to allow for the revised geometry (McCarthy et al. 2008).

This process is effective even in small groups. Indeed, it seems to be too effective when incorporated into a cosmological self-consistent model for galaxy formation and evolution. The current challenge is to realistically incorporate the mechanism into cosmological galaxy formation models. Current schemes seem to predict that the mechanism is rather too effective compared to the observational data.
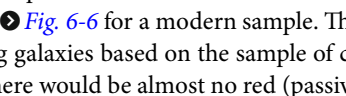
## 2.6 Evolution of Galaxy Clusters

The idea is appealing and simple. In order to map out the formation of cluster galaxies, we should find clusters at high redshift and compare them to local systems. The process has been likened to understanding the family history through a set of snapshot photographs. Of course, it is not quite so simple since we cannot observed the same cluster at different moments in its history, and we must piece the story together from statistical arguments.

It therefore needs care: (1) we need to match the masses of galaxies, not their luminosities, and to be careful to make measurements the rest frame of each cluster. (2) Massive clusters at high redshift will grow in mass by the present-day. They are also so rare that it can be problematic to sample a sufficiently large volume in the local universe. (3) We must pay attention to how the clusters are selected. If selection is based on an observed-frame optical band, high-z clusters will be preferentially selected if they contain more blue galaxies.

2.6.1 Color Evolution

One of the most striking results from the early observations of clusters was the Butcher–Oemler effect (Butcher and Oemler 1984). The authors reported the colors of galaxies in optically selected distant clusters. To the surprise of the community, they discovered a rapidly rising fraction of blue galaxies in the clusters. This was unexpected in that the effect was seen out to quite moderate redshifts ($z = 0.5$), in stark contrast to the paradigm of the time that cluster galaxies were old, with ages comparable to that of the universe.

The result is illustrated in ❯ *Fig. 6-6* for a modern sample. The line illustrates the evolution in the fraction of star-forming galaxies based on the sample of clusters at $z < 0.3$. If the trend could be extrapolated, then there would be almost no red (passive) galaxies in clusters at $z \sim 1$.
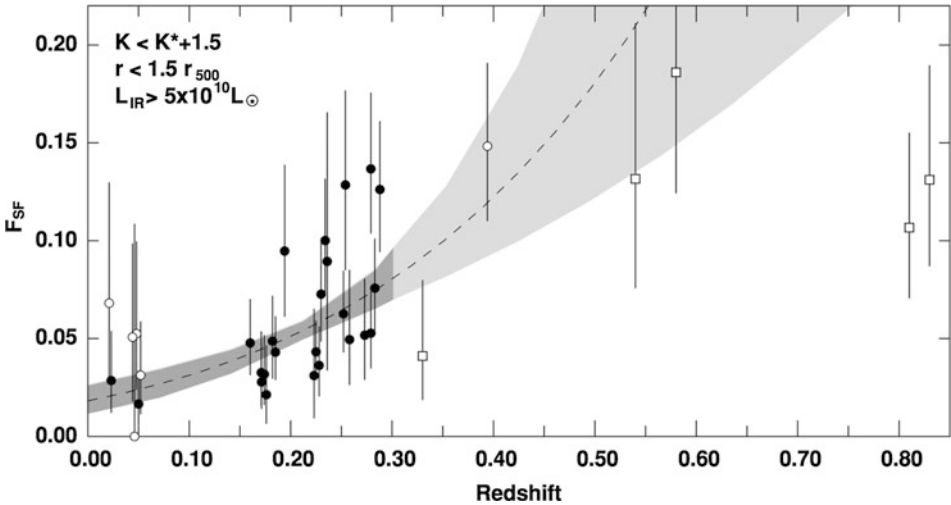
◨ **Fig. 6-6**

A modern measurement of the Butcher–Oemler effect. The Butcher–Oemler effect was originally seen as an increase in the fraction of blue (and hence star forming) galaxies in clusters towards higher redshifts. Here, the same effect is seen in a sample of carefully selected clusters using mid-infrared observations to identify star-forming galaxies. A rapid increase with redshift is suggested (*dashed line*, fitted to data z < 0.3), but scatter between clusters is very large. *Solid symbols* show results from high X-ray luminosity clusters, while *open symbols* denote systems of lower X-ray luminosity. *Open squares* show higher redshift clusters observed by Saintonge et al. (2008). Clearly, these clusters do not follow the trend suggested by the *dashed line* (Image credit: Haines et al. 2009)

Butcher–Oemler's original result has been heavily criticized. Clearly, not all the clusters follow the same trends, and some local but less relaxed clusters have blue fractions comparable to clusters at higher redshifts. Moreover, Butcher and Oemler's original selection of the clusters was inhomogeneous, with some of the clusters being selected from blue photographic plates. Clearly, this could bias the cluster sample to systems that contained more blue galaxies than the ensemble average. Another important bias is that the greater star formation rates of high-redshift field galaxies, combined with the bluer rest-frame pass bands typically used, mean that magnitude limited samples typically contain disproportionately many dwarf galaxies compared to local systems.

However, these biases do not seem to be sufficient to fully account for the effects, and the result has been reported in more modern cluster samples including results based on mid-IR star formation rates, as shown in the figure. It seems that these biases cannot fully explain the effect.

However, another bias is much harder to remove. Because the universe is younger (and the masses of clusters are more extreme compared to the average halo mass), the growth rates of clusters are significantly higher in the past compared to the present-day. Infalling galaxies cannot easily be distinguished from the virialized cluster population. Moreover, the field galaxy population is much more active at higher redshifts, with a larger fraction of the population

having blue colors. The situation is therefore unclear, and a modern interpretation could be that the increase in active galaxies results from the changes in the field galaxy population rather than from changes in the physics that occur within galaxy clusters.

2.6.2 E+A Galaxies

In the classic literature, the discussion of the evolution of cluster galaxies is closely related to the presence of a "new" population of "post-starburst" galaxies in distant clusters. These galaxies are often referred to as "E+A" galaxies because their distinguishing feature is spectra that are dominated by strong Balmer absorption, most notably the $H\delta$ line. The line strengths, combined with the absence of emission lines, seen in some spectra cannot be reproduced with declining star formation history. The best described as the spectrum of an A star superposed on that of an elliptical galaxy (hence the tag "E+A") and required a strong burst of star formation followed by an abrupt truncation (Couch and Sharples 1987). Recently, it has been realized that an alternative interpretation is possible in which the star formation is ongoing but heavily dust obscured. Only the A star population escapes from the strong dust obscuration creating the strong absorption.

The E+A population is now realized not to be confined to clusters, and examples of the E+A type are evident in the local galaxy populations where they can be observed in detail to explore the cause of the unusual activity. It is likely that the population originally identified in distant clusters is the result of the greater star formation rates of field galaxies and the subsequent suppression of their star formation in the cluster or galaxy group environment.

2.6.3 Cluster Archaeology

An alternative approach to cluster evolution is to observe the properties of local galaxies in detail. High signal-to-noise observations of galaxies in local clusters allow the degeneracy between metalicity and average stellar age to be broken. This work requires great care and the development of spectral models that allow for nonsolar element abundances.

While these results show that the high-mass cluster galaxies are old, as expected, they reveal a significant trend for the lower mass galaxies to be younger (❷ *Fig. 6-7*). This is an intriguing result that seems to require a degree of co-ordination between the metalicity of the lower mass galaxies and their weighted age. This cancelation does not arise naturally in theoretical models that have efficient feedback.

2.6.4 The Luminosity Function

A fourth approach to the evolution of cluster galaxies is to observed the system luminosity function. This requires care since the normalization of the luminosity (or mass function) depends on the overall mass of the halo and not the volume surveyed. To compare, the mass of the halo requires an independent measure of the system mass, such as that obtained from gravitational lensing.

However, the relative shapes of the mass function can be compared much more simply. In particular, the fraction of the total stellar mass contributed by high, and low-mass passive
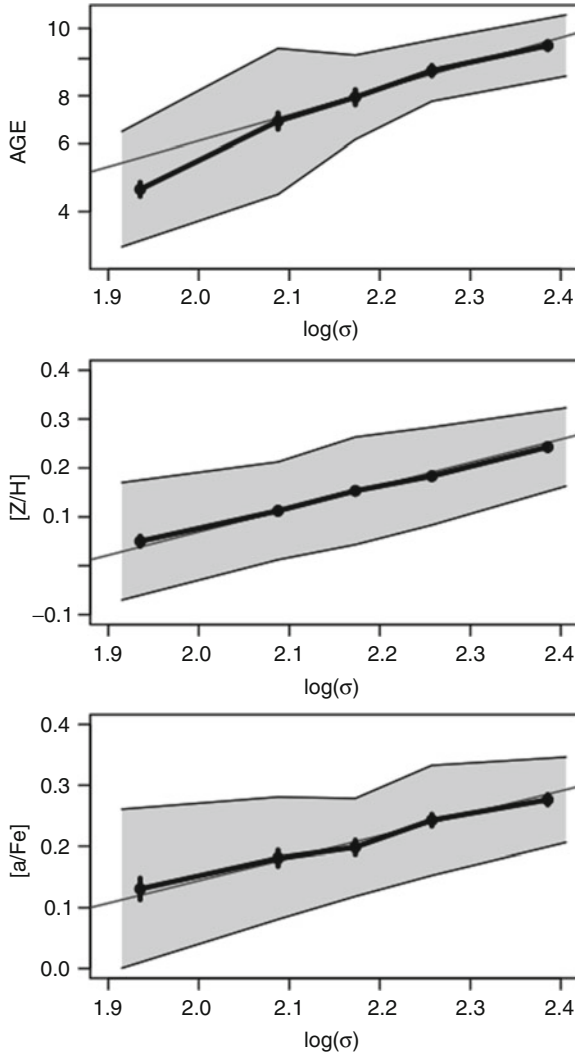
◼ Fig. 6-7
The dependence of age and metal abundance on galaxy velocity dispersion (effectively system mass) for a large sample of nearby early-type galaxies. The *thick line* shows the average age, metallicity, and *α* element enhancement. The *grey-shaded* region indicates the intrinsic scatter about the mean trend (Image credit: Nelan et al. 2005)

galaxies has proved to be a useful diagnostic and one that can be robustly measured. De Lucia et al. (2004) reported a relative porosity of low-mass red-sequence galaxies on the basis of HST imaging. The result has been confirmed in several (although not all) subsequent studies, such as that shown in ❯ *Fig. 6-8*.

It is interesting to compare this with the emergence of relatively young ages for low-mass galaxies from cluster archaeology. A simple interpretation suggests that the correlation between
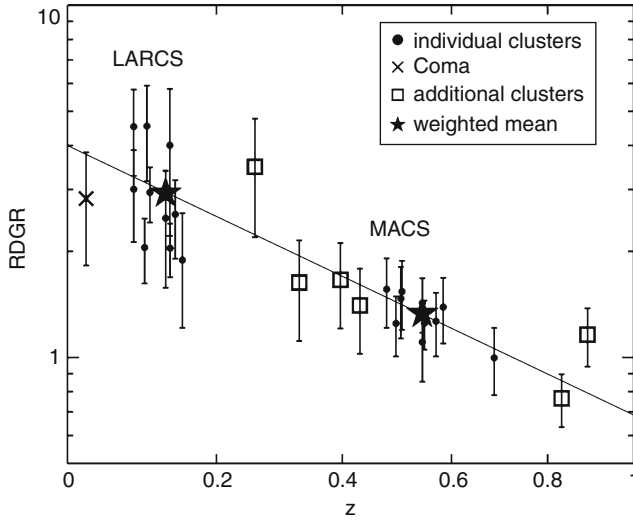
Fig. 6-8

The evolution of the ratio of dwarf (fainter than M_V = 20) to giant (brighter than M_V = 20) red-sequence galaxies as a function of redshift. The sample shown here is taken from Stott et al. (2007) and uses carefully matched samples of X-ray-selected clusters. A strong trend is seen with fewer red-sequence dwarf observed in the higher redshift clusters. This suggests that star formation in faint galaxies has not yet been suppressed in these systems

age and stellar mass should twist the color-magnitude sequence, increasing its slope at higher redshift (in contrast to the mild slope evolution that is observed). However, this is based on the assumption that the star formation rate slowly declines as the galaxy is incorporated into the clusters. A more complex interpretation appears to be required, in which galaxies make a rapid switch between the passive and star-forming sequences. It is interesting to note that the "rapid switch" picture is supported by the strong presence of two sequences even in studies of the group and field population (Balogh et al. 2004).

The discussion of the evolution of the stellar mass function has highlighted the need for care when comparing clusters at different redshifts and even between systems of different mass. It is now very apparent that stellar masses need to be compared on a like-for-like basis and that samples need to be compared on the basis of stellar mass, not luminosity (particularly luminosity in bluer bands). This not only complicates the comparison of systems at different redshift, but it makes it harder to compare systems of different total halo mass (since this also affects the stellar mass function).

2.6.5 Morphology

The launch of the HST has offered the possibility of studying the morphologies of galaxies in distant clusters, allowing this to be compared to the changes in the star-forming properties. This topic has resulted in extensive controversy largely because of the difficulty in obtaining

objective computer-derived morphologies. Carefully moderated "eyeball" morphologies consistently suggest that distant clusters contain fewer S0 galaxies and more spiral galaxies than local counterpart clusters (Dressler et al. 1997). Interestingly, the clusters contain similar fractions of early-type galaxies at all redshifts, hinting that the cluster population consists of an intrinsic elliptical galaxy population and an S0 population that has built up over time. It is difficult to reproduce this result, with current galaxy formation models.

The spiral to S0 transformation would appear to reinforce the evolution of galaxy colors first suggested by the Butcher–Oemler effect. However, the same caveats about the role of magnitude limits, cluster selection, and galaxy infall apply equally here. Nevertheless, many authors are convinced of the evidence for a long timescale of transformation of spiral galaxies to S0, others identify galaxy groups as the key environment in the history. Care, however, needs to be exercised since many studies average the whole galaxy population together and do not fully account for the biases in the stellar mass function of cluster, group, and isolated galaxies.

2.6.6 Other Wavebands

Observations in the FIR have opened up the possibility of including deeply dust-obscured star formation in the census of star formation in clusters and groups of galaxies. In particular, the observations stand to reveal a source of star formation in the E+A galaxy population.

To date, the results have been mixed. Some authors report the discovery of strong FIR sources in clusters, consistent with such deeply obscured star formation (Geach et al. 2009). However, the sources appear to be rare, and when the mass biases are taken into account, it is unclear whether the population is specific to the cluster environment, or is better accounted for by the enhanced infall of cluster galaxies. With the advent of Herschel and better models for the evolution of galaxies, this is a rapidly advancing field.

2.7 The Relation of Clusters to Galaxy Groups

The above discussion makes it clear that the evolution of galaxy clusters cannot be separated from the evolution of galaxy groups and a great deal of effort is being targeted on measuring the properties of galaxies in less rich environments, or even to measure the properties of galaxies as a function of their clustering strength rather than assigning individual halo masses to galaxies. The later approach has the advantage that it can be computed using objectively defined statistical measures such as the correlation function or the marked correlation function.

Studies of galaxy groups are, however, hard work compared to studies of clusters since targetted spectroscopic campaigns return a much larger fraction of field galaxies compared to group members. One of the best approaches is therefore to undertake large, highly complete redshift surveys (such as the zCOSMOS survey (Maier et al. 2009)) and to select galaxy groups from the survey. These can then be followed up in more detail. The results are exciting – at intermediate redshift, the galaxy groups are offset from the field but have a larger proportion of active galaxies than similarly selected groups at low redshift. These results are now being confirmed out to higher redshifts. At $z = 1$ groups from the zCOSMOS survey appear to be dominated by a transition population of E+A galaxies (Balogh et al. 2011). These results have encouraged many authors to consider that galaxy groups are the powerhouse of galaxy transformation.

Another approach to this issue is to assign each galaxy an environment based on its local density. Peng et al. (2010) use this approach to present an interesting view of the relation between galaxies and environment. Presenting the results in this was, they show that the fraction of star-forming galaxies can be effectively written as the product of two quenching terms, one based on the galaxy's mass and the other on its local density. The two terms are independent, which seems to agree well with the expectation of theoretical models. This will be an interesting angle to pursue with new, even larger, redshift surveys.

2.8   Intra-cluster Light

In a later section, I will present the role of dynamical friction in causing the orbits of galaxies to decay. As the orbit decays, the galaxy becomes subject to stronger tidal forces which may strip stars from the outer parts of the galaxy. The stars that are stripped in this way would continue to orbit in the cluster creating a diffuse interstellar glow. Although faint, the diffuse light is just observable (Gonzalez et al. 2005), particularly around the dominant galaxy where it is concentrated to the center of the gravitational potential.

Although the existence of the intra-cluster light is now well established, The total fraction of stars in this diffuse form is still a matter of controversy. It is difficult to make this assessment directly because of the surface brightness that drops rapidly away from the central galaxy. McGee and Balogh (2010) circumvent this difficulty by measuring the intergalactic supernova rate in clusters. Current estimates suggest that the intra-cluster light in clusters accounts for about 10% up to 50% of the total star light. While recent measurements in lower-mass haloes have suggested a larger contribution (based on extrapolation to low surface brightness), it is hard to see how these results can be reconciled with the hierarchical growth of massive clusters from lower mass systems.

3   X-Ray Emission

3.1   The Physics of X-Ray Emission

The optical properties of galaxy clusters reflect only a small fraction of their baryonic mass. Most of the baryons in a cluster are in the form of a diffuse intra-cluster medium (ICM). This relatively dense, high-temperature plasma gives rise to copious X-ray emission. The typical temperature of the cluster plasma is 10^7–10^8 K, and the core density reaches 0.01–0.1 atoms per cm^{-3}. At these temperatures, the plasma is highly ionized leading to X-ray emission from thermal Bremsstrahlung (also referred to as free–free emission) and inner-shell electron capture and transitions.

3.1.1   Thermal Bremsstrahlung Emission

Conceptually, thermal Bremsstrahlung is straightforward. It arises as the trajectories of electrons are deflected by the strong fields of ionized nuclei, including H^+ and He^{++}. The acceleration of the electron generates the emission of a photon. Computation of the actual spectrum

involves integration over impact parameters and the thermal distribution of electron velocities. For an ion with charge Z and a plasma with electron temperature T_e and electron and ion densities n_e and n_i, respectively, the emissivity (per unit volume per unit frequency) is given by

$$\epsilon_Z^{ff}(\nu) = A_Z n_e n_i T_e^{-1/2} \exp(-h\nu/k_B T_e) \tag{6.6}$$

where k_B is the Boltzmann constant, h Plank's constant, and the normalization constant is given by

$$A_Z = \frac{2^5 \pi e^6}{3 m_e c^3} \left(\frac{2\pi}{3 m_e k_B} \right)^{1/2} Z^2 g_{ff}(Z, T_e, \nu) \tag{6.7}$$

where m_e is the electron mass, e the electron charge, and g^{ff} the Gaunt factor, a slowly varying function that corrects quantum mechanical effects (Sarazin 1988).

The spectrum has a continuous exponential distribution. If plotted in terms of $\log(\nu)$, this translates to a break at high energies corresponding to the thermal temperature of the plasma. In order to obtain the total luminosity arising from free–free emission, we must integrate over frequency and the volume, V, of the cluster and sum over each species:

$$L^{ff} = \sum_Z \int_\nu \int_V \epsilon_Z^{ff}(\nu) \, d\nu \, dV \tag{6.8}$$

Although the emission formula appears complex, it is characterized by its dependence on the square of the density of plasma and its $T_e^{1/2}$ temperature dependence. The later arises because a higher temperature pushes the photon energy cutoff to higher energy ($\propto T_e$), while the higher temperature reduces the effectiveness of individual collisions ($\propto T_e^{-1/2}$). Free–free emission in spectrum is dominated by collisions with hydrogen and helium nuclei.

The dependence on the square of the plasma density is a key result. This has important consequences for the cooling instability since most heating mechanisms depend linearly on density. This makes it difficult for a heating mechanism to simultaneously compensate for radiative cooling over a range of radii.

Thermal Bremsstrahlung dominates the emissivity at temperatures above 8×10^7 K, where the common elements become completely ionized. At lower temperatures, electron energies are comparable to the ionization potential and free-bound and bound–bound transitions become important.

3.1.2 Bound–Bound Electron Transitions

X-ray emission also arises from bound transitions and the capture of electrons into bound shells. Typically, the electron will be captured into a high-energy state, and a cascade of X-ray transitions will result. Alternatively, one of the ion's inner-shell electrons will be excited by collisional processes. The resulting spectrum of emission lines depends both on the temperature of the plasma and the abundance of different species. The calculation is complex because it requires careful determination of the ionization balance of each species. More details of the calculation are given in Sutherland and Dopita (1995). Recent calculations of the emission spectrum are discussed in Wiersma et al. (2009), where the role of photo-ionization is considered in depth. Fortunately, this correction is less important for high-temperature plasmas such as those in clusters. Line emission dominates the emissivity at temperatures below 10^7 K.
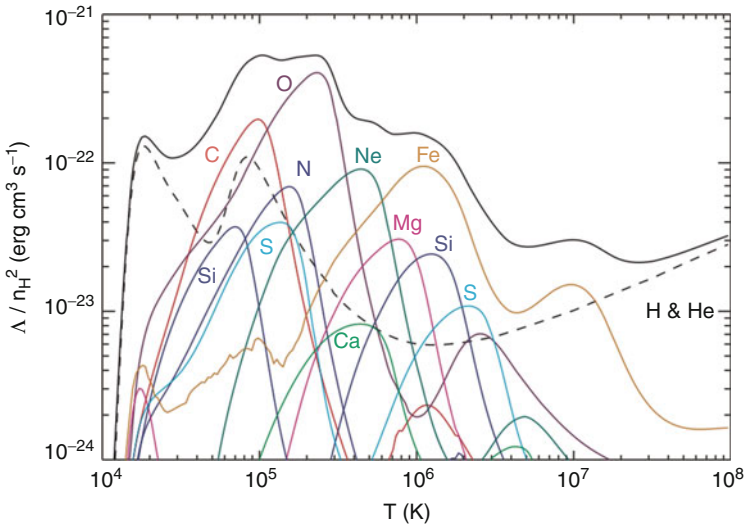
◼ Fig. 6-9
The contribution of different elements to the overall cooling rate of the intra-cluster plasma. The plot here illustrates the temperature dependence of the total emissivity for a solar abundance plasma (*solid lines*). The contributions of different elements are indicated. The emissivity of a primordial plasma containing on hydrogen and helium is indicated by a solid line. These calculations assume that the plasma is in collisional ionization equilibrium, and at low temperatures, the cooling curve is modified substantially in the presence of an ionizing background (Image credit: Wiersma et al. 2009)

Just as for thermal Bremsstrahlung, the total emissivity depends on the square of the plasma density since ionization mechanism is (at cluster temperatures) a two-body process. Moreover, the shape of the emission spectrum can be used to infer the plasma temperature and the abundance makeup. If the relative abundance of the elements is known, this makes it possible to accurately infer the density and temperature of the plasma even in relatively low-quality X-ray data (❷ *Fig. 6-9*).

It is interesting to consider the temperature dependence of the total (or volumetric) emissivity in more detail. For a plasma that has not been enriched by stellar nucleosynthesis, the temperature dependence of the total emissivity is dominated by two peaks corresponding to the ionization potentials of hydrogen and helium. As the metal abundance of the plasma increases, the elements C, O, and Ne play an important role. As a result, the total emissivity of the plasma has a very strong dependence on metal enrichment in the temperature range 10^5–10^7 K. This has important consequences for the predicted luminosities of groups and clusters. Cross talk between the formation of stars and the cooling of gas in galaxy clusters makes simulations of the universe extremely challenging.

In addition, nonthermal processes can also lead to the emission of higher energy photons. The comptonization of the cosmic microwave background, in particularly, is potentially important at higher redshift.

3.1.3 Total Emissivity

The total (or volumetric) emissivity is conveniently written as

$$\epsilon = n_H^2 \Lambda(T, Z) \tag{6.9}$$

where n_H is the hydrogen number density and Λ encapsulates the complex function of temperature and ion abundance. This must be computed with computer codes such as those of Sutherland and Dopita (1995) and Wiersma et al. (2009). Tabulated results are readily available, but care needs to be taken to ensure that the density term in (❷ 6.9) is consistently defined; many authors use a pre-factor of $n_e n_H$. For a primordial plasma containing 25% helium by mass, $n_e = 1.167 n_H$. Fortunately, the gross behavior of the emissivity can be approximated by

$$\Lambda \approx 3 \times 10^{-23} (T_8^{1/2} + 0.5 f_m T_8^{-1/2}) \, \mathrm{erg \, cm^3 \, s^{-1}} \tag{6.10}$$

where T_8 is the plasma temperature in units of 10^8 K and f_m is a factor that takes into account the metal abundance of the plasma (Peacock 1999). For solar abundances, $f_m = 1$, and for a primordial plasma, $f_m \approx 0.03$. Note that at high temperatures, we recover the $T^{1/2}$ dependence expected for thermal Bremsstrahlung, while at temperatures lower than those of groups and clusters, the dependence is $T^{-1/2}$.

3.2 The Baryon Content of Galaxy Clusters

We can apply our understanding of the emission mechanisms to determine the hot gas content of galaxy clusters. The temperature can be inferred from the spectrum. If consideration is restricted to fixed element abundance ratios, this can be achieved even at relatively low spectral resolution. This makes it possible to construct detailed temperature (and abundance) maps for nearby clusters.

3.2.1 Temperature and Density Profiles

The temperature profile is close to isothermal, with most clusters showing a modest decrease in temperature towards their center, and a slight drop in temperature towards their outer edge. The temperature of the system can be estimated from the Virialized mass, M_v, of the object

$$k_B T = \frac{1}{2} \mu m_p V_c^2 \tag{6.11}$$

where μ is the average particle mass (0.59 for a primordial plasma), m_p is the proton mass, and V_c is the circular velocity of the halo, defined as

$$V_c = G^{1/2} M_v^{1/3} \left(\frac{4\pi}{3} \rho_v \right)^{1/6} \tag{6.12}$$

where ρ_v is the average density of the halo. Typically, we assume $\rho_v = 200 \rho_{\mathrm{crit}}$, where ρ_{crit} is the critical density of the universe at the redshift of collapse. Combining these expressions, we expect a mass–temperature relation close to

$$T \approx 1.6 \times 10^7 \left(\frac{M_v}{10^{14} \, M_\odot} \right)^{2/3} \mathrm{K} \tag{6.13}$$

This is within 15% of the observed relation (Vikhlinin et al. 2006).

The density can be reconstructed from the observed X-ray surface brightness. Of course, care is needed to reconstruct the 3-dimensional density distribution from the 2-dimensional measurements. This typically involves making an assumption of spherical symmetry which allows the contribution from successive shells to be determined.

Clusters are conventionally fitted by a density profile of the form

$$\rho = \frac{\rho_c}{(1 + (r/r_c)^2)^{\frac{3}{2}\beta}} \tag{6.14}$$

where ρ_c, r_c, and β are fitting constants. Typically, $\beta = 2/3$ provides an adequate fit although more recent papers fit more complex profiles, or dispense with simple fitting formulae altogether and use the results of numerical simulations directly (Vikhlinin et al. 2006). Central gas densities greater than 10^{-2} atoms per cm^3 ($\rho_g \sim 3 \times 10^{14}\, M_\odot\, Mpc^{-3}$) and core radii around 100 kpc are typical. The plasma is typically enriched with metals, typically to about 1/2 of the solar abundance (Leccardi and Molendi 2008).

Integrating the profile gives the total gas mass. This is typically 12% of the total system mass (see below for a discussion of techniques for estimating the total mass of the system). The gas content of clusters is much greater than the mass in stars and in cold gas, which makes up only 10% of the total baryon content. A great deal of the residual uncertainty comes from the diffuse intra-cluster stars.

These fractions are very comparable to the stellar fraction of the universe as a whole, with the notable exception that it is not possible to directly detect intergalactic plasma because its temperature is too low for efficient X-ray emission and its presence is inferred indirectly from cosmological measurements of Ω_b/Ω_m.

3.2.2 The Entropy Distribution

Measurement of the temperatures and density of the intra-cluster plasma may be summarized in terms of the "entropy" of the plasma at each radius. Typically, X-ray astronomers use the adiabat of the gas

$$K \equiv k_B T \rho^{-2/3}$$

as a proxy for the entropy (thermodynamic entropy is proportional to $\log K$). The adiabat is a useful quantity, because it does not change as the gas is adiabatically compressed due to changes in the gravitational potential. Moreover, the buoyancy of the gas results in a natural sorting of the material such that the lower entropy material sinks to the center of the cluster, while the higher entropy material rises to the outside. Numerical experiments show that this segregation occurs rapidly as the cluster grows. Hydrostatic equilibrium, buoyancy, and an insensitivity to the outer boundary conditions make it possible to uniquely specify the gas distribution in the cluster in terms of the gravitational potential and the entropy distribution.

Entropy also provides a good variable for cluster studies since it can be used to infer the total heating and cooling of the gas as the system has formed. Heating sources include the shock heating of gas as it enters the cluster (and energy injected by a central radio galaxy), while cooling is dominated by the radiative losses of the ICM. These ideas can be used to treat clusters
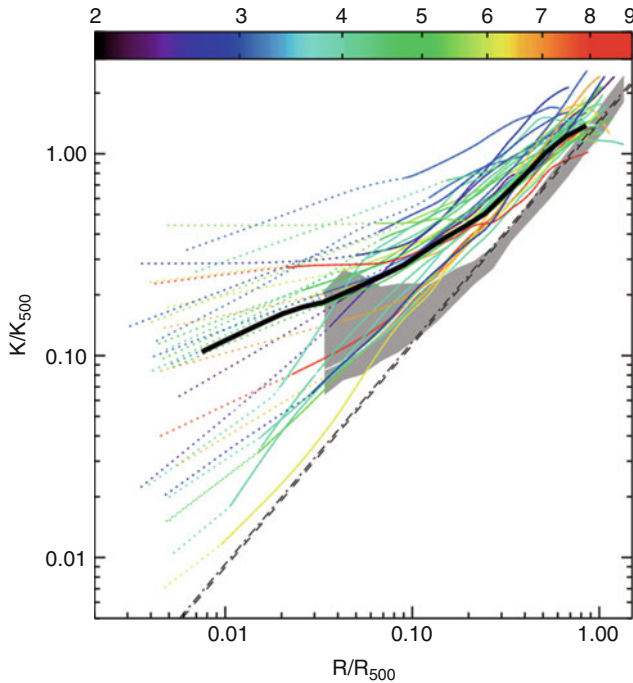
◼ Fig. 6-10
The entropy profiles of intra-cluster medium in galaxy clusters taken from the REXCESS survey. The entropy profile in each cluster has been scaled by dividing by the characteristic entropy expected for a cluster of the observed temperature $\left(K_{500} = \frac{1}{2} \left(\frac{2\pi G^2 M_{200}}{15 f_b H(z)} \right) \right)$**. The colors of the** *lines* **indicate the cluster temperature.** *Black lines* **and** *shaded regions* **show the expectations of theoretical models. Scaling by** K_{500} **brings the profile to similar values at the outer edge of the system, but the profiles have a wide range of slopes. Typically, the lower temperature clusters have shallower profiles. This results from a loss of the lower entropy material from these systems (Image credit: Pratt et al. 2010)**

of galaxies as "cosmic calorimeters" allowing us to gain great insight into the thermal history of the material that is left over from the process of galaxy formation (❯ *Fig. 6-10*).

Observations of the entropy distribution functions of clusters of different mass reveal an unexpected scaling. Rather than the entropy distributions being scaled copies of each other, gas in lower mass systems has a much flatter distribution of entropy. This leads to a much lower concentration of the central gas and hence to much weaker X-ray emissivities of low-mass clusters than expected. The difference cannot be attributed to a greater stellar fraction in the lower mass systems, but the distinction is clearly connected to the "cooling flow paradox" that we discuss below. Initially, the differences in entropy profile were thought to result from a minimum entropy boost associated with an early epoch of galaxy formation (Ponman et al. 1999), but it now seems more appropriate to view this as arising from the loss of low entropy material from lower mass groups during the cluster formation (McCarthy et al. 2011). This has provided powerful but complimentary evidence for the role of AGN in regulating the formation of galaxies.

3.3 The Cooling Instability

A useful quantity is to define the cooling time of the X-ray plasma as the ratio of its thermal energy to its radiation rate:

$$t_{\text{cool}} \equiv \frac{\frac{3}{2} n \, k_B T}{n_H^2 \Lambda} \tag{6.15}$$

where n is the total number of thermal particles in the plasma and n_e and n_H are the electron and hydrogen number density of the plasma. For a primordial plasma containing 25% helium by mass, $n = \frac{\rho_g}{0.59 m_p}$ and $n_H = \frac{\rho_g}{1.33 m_p}$, where m_p is the proton mass and ρ_g is the plasma density. Using the approximation for Λ introduced previously (❯ 6.10), one obtains

$$t_{\text{cool}} \sim 16 \left(\frac{\rho_g}{(10^{14} \, M_\odot \, \text{Mpc}^{-3})} \right)^{-1} \left(T_8^{-1/2} + 0.5 f_m T_8^{-3/2} \right)^{-1} \text{Gyr} \tag{6.16}$$

Inserting a typical core gas density and temperature gives $t_{\text{cool}} \sim 3$ Gyr, significantly shorter than the age of the universe.

The key point is that denser plasma has a shorter cooling time. Reducing the temperature also shortens the cooling time. This leads to a cooling instability. As the plasma radiates, it is squeezed by the weight of the material at larger radii. The net effect is that the pressure remains roughly constant, but the density rises. The rise in density further increases the emission rate, which in turn accelerates the increase in density. This leads to a radial inflow of gas referred to as a "cooling flow" (Fabian 1994). Initially, the rate of flow is much smaller than the system sound speed, and it is adequate to consider the cluster proceeding through a sequence of quasi-hydrostatic states. Eventually, this approximation breaks down, and the plasma becomes subject to local instabilities that grow on a timescale comparable to the free-fall time of the gas.

Clusters of galaxies are thus intrinsically unstable (❯ *Fig. 6-11*), leading to the expectation that the observed cluster should contain a net inflow of material towards the center of the gravitational potential. Fortunately, the timescale for such flows in clusters is relatively long compared to the overall age of the universe. Nevertheless, while we would not expect the cluster to cool completely, a significant fraction of the material is expected to flow towards the center of the system. Paradoxically, there is no evidence for such "cooling flows" on the scale expected.

A subtle but important point is that the cooling of the plasma does not necessarily result in a drop in temperature if the cooling time is longer than the system dynamical time. In a quasi-hydrostatic, flow the temperature reflects the shape of the potential. However, once the gas is sufficiently dense, the cooling time becomes short compared to the dynamical time and clumps of gas will condense out of the flow and cool.

In contrast to the situation in galaxy clusters, the cooling time is relatively short in galaxy systems. A relevant comparison is with the local dynamical time:

$$t_{\text{dyn}} = \left(G \rho_{\text{tot}} \right)^{-1/2} \tag{6.17}$$

where ρ_{tot} is the total density (including both dark matter and gas). Assuming $\Omega_b / \Omega_m = 0.167$ and that dark matter and gas have the same distribution (a poor approximation within clusters!), we can write

$$t_{\text{dyn}} \approx 2 \left(\frac{\rho_g}{10^{14} \, M_\odot \, \text{Mpc}^{-3}} \right)^{-1/2} \text{Gyr} \tag{6.18}$$

Comparing this with (❯ 6.16), $t_{\text{cool}}/t_{\text{dyn}} \gg 1$ in the centers of galaxy clusters. However, the ratio rapidly declines as the virial temperature of the halo falls, and the way in which cooling proceeds
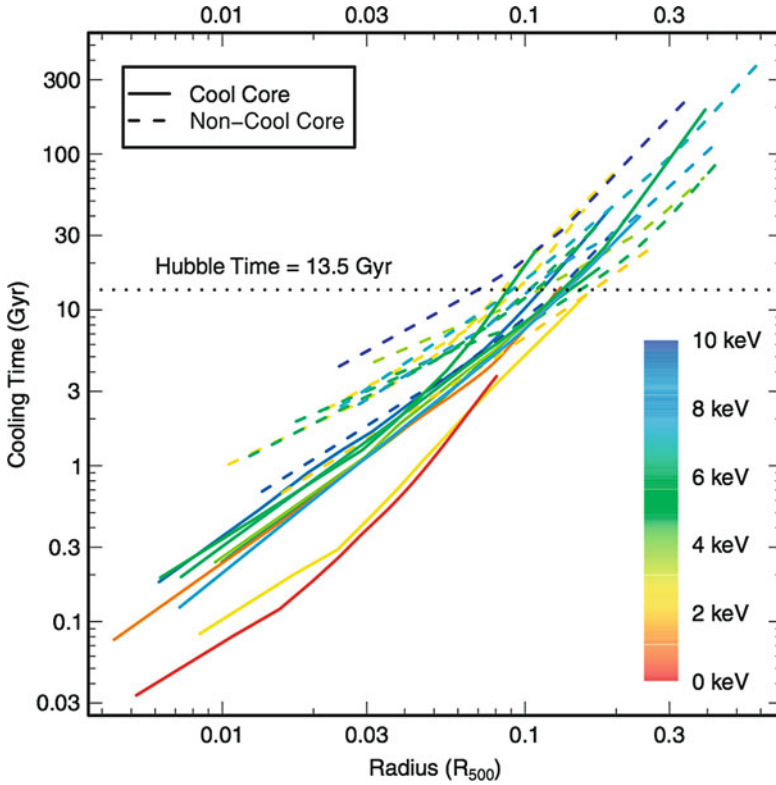
▣ **Fig. 6-11**
The cooling time profiles of a sample of X-ray clusters taken from Sanderson et al. (2006). The cooling time of the plasma decreases strongly with decreasing radius so that the central cooling time of most clusters is much less than the age of the universe. *Solid* **and** *dashed lines* **distinguish between clusters that have a central dip in their temperature profile and those that do not (Image credit: Sanderson et al. 2006)**

in galaxy-scale haloes is potentially quite different to that in higher mass cluster systems (White and Frenk 1991; Dekel and Birnboim 2006). This leads to an important distinction between hot-mode accretion (i.e., cooling flows) and the "cold-mode" accretion that dominates the growth of galaxies. In galaxies, the fueling rate is therefore determined by the rate of growth of the halo and not the rate at which gas is able to radiate its energy. The accretion rate of galaxies is thus a strong function of redshift.

Is strong AGN feedback in clusters inevitable, or should we be surprised by the frequency and strength of the energy input? This is currently a subject of much debate. On the one hand, if the AGN were not present or effective, this would lead to a pileup of cold gas at the center of the cluster. Surely, this would eventually lose its angular momentum and find a way to accrete onto the central black hole and thus establish a regulating feedback loop! But while this picture is appealing, there are many missing pieces. For example, why are the processes so effective at transporting the cooling gas down to a few Au of the black hole? What would happen if the accretion rate were so high that the central accretion disk radiated the accretion energy away

rather than producing a powerful radio jet? Hopefully, we will be able to piece together a much more complete picture in the near future.

3.3.1 Cooling Flows: Comparison to Observations

Detailed calculations of the cooling time profiles of galaxy clusters suggest that material should be flowing to the center at typical flow rates of 100–1,000 $M_\odot$year^{-1} (Peres et al. 1998). The rates are sensitive to the resolution of the X-ray observations (higher flow rates are found in better resolved systems), and samples are biased by X-ray selection (since clusters with higher cooling rates also have higher X-ray luminosity). Nevertheless, this work leads to the expectation that, in the absence of an effective heating mechanism, mass should be transported to the center of the cluster, cool out and form into stars. Some modern determinations of cooling time profiles are shown in ❯ *Fig. 6-11*.

However, the short cooling times seem contrary to observations.

(1) Although central cluster galaxies often contain significant populations of young stars and cold gas, the inferred star formation rates are roughly 1/10 of that inferred from the analysis above. Similarly, the observation of extended Hα emission filaments does not directly imply the high star formation rates since the emission strength greatly exceeds that expected even under the flow scenarios above. It seems more likely that the filamentary emission is indicative of the cosmic ray flux in the cluster.

(2) As gas cools in the cluster, it should be possible to identify multiphase gas including components with temperature well below the mean plasma temperature. A low-temperature component would however emit efficiently in low-ionization lines. Surprisingly, these are not evident in the X-ray spectrum of clusters (Peterson et al. 2003), limiting the maximum cooling rate to less than 10 $M_\odot$year^{-1} in typical systems.

Many clusters are observed to have a central dip in temperature. Although this is often assumed to be a result of high cooling rates, the temperature of the plasma more accurately reflects the underlying gravitational potential. In gravitating systems, cooling (energy loss) does not result in a drop in temperature.

3.3.2 Resolution

The lack of evidence of a sink for the cooling material has led to the search for an energy source to offset the radiated energy. If there is sufficient energy input, the system can be held in (or close to) a steady state. It has been apparent for some time that clusters of galaxies are often associated with radio sources, but the significance of this association has only recently become clear (Binney and Tabor 1995; Churazov et al. 2001; Fabian et al. 2006). It is now widely accepted that heat input from radio galaxy activity (ultimately from the accretion of mass onto a central black hole) provides the energy source that offsets the cooling losses from the ICM.

Radio galaxies are driven by AGN activity, but the activity is usually only visible through the radio frequency emission produced by the synchrotron radiation of relativistic electrons. In contrast to Quasars and Seyfert galaxies, optical line emission from the central black hole may be weak or absent. Radio observations classify such radio galaxies into FRI or FRII morphologies depending on the relative brightness of the central source compared to the hot spots at the end of the radio lobes. Clusters usually host FRI galaxies.

The classification and study of radio galaxies is a vast subject in its own right. For our purposes, we will focus on radio galaxies as a source of energy in the cluster. It should be emphasized that the power directly measured in the radio emission is small. However, it has recently been seen that the radio jets correspond to cavities in the X-ray surface brightness. This allows the total power to be estimated directly from the PV work done in displacing the ICM. The current paradigm is that the radio jet inflates a bubble that then raises in the cluster due to its buoyancy (Churazov et al. 2001). As it rises, its buoyant energy is dissipated in the surrounding medium. Additional heating may come from weak shocks as the bubble is inflated.

Observationally, the mechanical luminosity, L_{mech}, is given by

$$L_{\mathrm{mech}} = \frac{\beta p_{\mathrm{icm}} V_c}{t_c} \tag{6.19}$$

where p_{icm} is the ambient pressure of the intra-cluster medium surrounding the cavity, V_c is the cavity volume (which must be estimated from its projected size), and t_c is the age of the cavity. β is a coefficient that accounts for the total work done as the cavity is inflated and rises: values between 3 and 10 are plausible. The age of the cavity t_c must be estimated from its buoyant rise time. Current estimates of the heating rate suggest that it is comparable to the cooling rate (❏ *Fig. 6-12*), and thus heating by radio galaxies may well resolve the "cooling flow paradox."
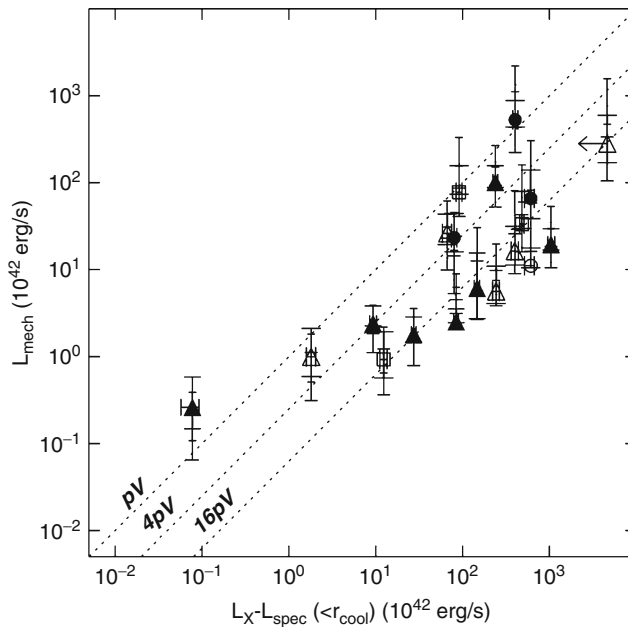
❏ **Fig. 6-12**
Comparison of the heating and cooling powers of a sample of galaxy clusters (Birzan et al. 2004). Cooling luminosities are calculated from the X-ray emissivity of the cluster, while heating power is derived from cavities in the X-ray emission. *Open* **and** *closed symbols* **differentiate systems in which the cavity is/is not filled with radio-emitting plasma. Diagonal** *dashed lines* **shows the total heating rate required to completely offset the cooling in each cluster (Image credit: Birzan et al. 2004)**

Detailed observations show that the shutdown of star formation is not complete, and central galaxies continue to form stars at rates of typically 1–10 $M_\odot \text{year}^{-1}$, with associated emission from molecular gas (Edge 2001). The lack of a complete shutdown is unsurprising, given the intermittency of the radio outbursts and the nonspherical nature of jet emission, but the star formation observed in central galaxies makes little contribution to the growth of the stellar system.

The feedback from radio galaxies clearly plays an important role in suppressing cooling flows and thus in establishing the maximum mass of galaxies that are formed (Bower et al. 2006). Incorporating these mechanisms into theoretical models greatly improves their ability to describe the observed universe. The action of the AGN activity may also play an important role in stirring the central gas, extending its central cooling time and distributing the metals ejected by the central galaxy.

3.4 The Sunyaev–Zeldovich Effect

The Sunyaev–Zeldovich (SZ) effect arises because the hot electrons in the intra-cluster plasma scatter cosmic microwave background photons to higher temperatures. This imprints a pattern of spots on the cosmic microwave background (CMB) at the location of clusters. Depending on the frequency of observation, the spot many be more or less luminous and this makes it possible to efficiently distinguish the clusters from intrinsic CMB fluctuations and other foreground. The detection of clusters through CMB methods is currently the subject of great attention: from the ground with the South Pole Telescope and from space with the Planck mission.

The effect of the cluster is often encapsulated by the comptonization y parameter:

$$y \equiv \int \sigma_T n_e \frac{k_B T}{m_e c^2} dl \tag{6.20}$$

At low frequencies, the SZ effect cause a decrease in the CMB intensity $\delta I/I = -2y$.

One of the advantages of the SZ effect is that the decrement does not depend on redshift. Furthermore, it does not depend on the detailed clumping of the IGM, since only the pressure is important. This means that it is a powerful alternative to exploring the properties of the IGM. This will be an important avenue for future work.

4 Dark Matter

One of the most important roles of galaxy clusters has been to provide conclusive proof of the existence of dark matter. Combined with limits on the abundance of baryons from nucleosynthesis and observations of the cosmic microwave background, this implies that the dark matter is non-baryonic. We consider three methods of measuring the dark matter content of clusters below.

4.1 Galaxy Dynamics

A gravitating system of bodies obeys the virial theorem:

$$2K_e + W = 0 \tag{6.21}$$

where K_e is the kinetic energy of the system and W is the potential energy:

$$K_e = \sum_i \frac{1}{2} m_i v_i^2$$

$$W = \sum_i \sum_{j>i} \frac{G M_i M_j}{|r_i - r_j|}$$

Observations of the cluster can provide estimates of the line-of-sight velocities of galaxies. Assuming spherical symmetry, $\sigma_{3D}^2 = 3\sigma_{los}^2$. This is equivalent to a plasma temperature of

$$T \approx 7 \times 10^7 \left(\frac{\sigma_{los}}{1,000 \text{ km s}^{-1}} \right)^2 \text{ K} \tag{6.22}$$

Similarly, the 2-dimensional distribution of the galaxies can be used to estimate the average inverse separation. For a r^{-2} density distribution,

$$\left\langle \frac{1}{r_i - r_j} \right\rangle \approx \frac{1}{0.6R}$$

where R is the virial radius of the system. Hence, the mass of the cluster can be estimated:

$$M \approx \frac{3 \langle \sigma_{los}^2 \rangle R}{G} \tag{6.23}$$

More accurate calculations must allow for orbital anisotropy and a variety of other effects.

4.2 Hydrostatic Equilibrium

The X-ray-emitting plasma permits another approach to mass measurement. Assuming spherical symmetry and that pressure forces balance the gravitational forces so that the system is in hydrostatic equilibrium, we have

$$\frac{1}{\rho_{gas}(r)} \frac{dP}{dr} = -\frac{GM(<r)}{r^2} \tag{6.24}$$

where $M(r)$ is the total mass enclosed within radius r and ρ_g is the gas density.

Since the intra-cluster plasma is well described by an ideal gas with mean molecular weight μ, the gas density and temperature are related to pressure by

$$P = \frac{\rho_g k T}{\mu m_p} \tag{6.25}$$

where our assumption of hydrostatic equilibrium means that turbulence makes a negligible contribution to the total pressure. For a pure ionized hydrogen plasma, $\mu = 0.5$, and for a more realistic plasma including helium and heavier elements, $\mu = 0.6$. Eliminating pressure from the equations gives

$$M(r) = -\frac{k_B T(r) r}{\mu m_p G} \left(\frac{d \ln T}{d \ln r} + \frac{d \ln \rho_g}{d \ln r} \right) \tag{6.26}$$

Since T and ρ_g can be mapped from the X-ray data, we can see that X-ray measurements of the 3-dimesional density and temperature profiles thus allow us to determine the total enclosed mass.

For a simple example, if the cluster is isothermal and the density profile is described by $\rho_g \propto r^{-2}$ (as appropriate for (❯ 6.14) at large radius), the enclosed mass is given by

$$M = \frac{2k_B T}{G\mu m_p} R = 6.5 \times 10^{14} \, M_\odot \left(\frac{T}{10^8 \, \text{K}}\right) \left(\frac{R}{1 \, \text{Mpc}}\right) \tag{6.27}$$

More complete analyses can make use of the full temperature and density profiles. Using simulations as a guideline, a 10% correction should be included to allow for departures from hydrostatic equilibrium. The error arising from departures from spherical symmetry can also be estimated in this way. The error tends to be small because the gravitational potential is more symmetric than the underlying gas distribution. High-quality X-ray measurements thus provide a robust means of determining the mass profiles of clusters.

4.3 Gravitational Lensing

Because of the high dark matter content of clusters, they create strong sources of gravitational lensing. These result in spectacular giant arcs. However, the use of gravitational lensing for cluster is more easily applied to the weak lensing case, where the lensing effect results in the weak distortion of background galaxies. The effect on an individual galaxy is weak, but by averaging over many galaxies, a clear signal can be obtained.

The underlying principle of gravitational lensing is that the gravitational potential of the cluster gives space an effective refractive index. This deflects light rays passing through the cluster. For a circularly symmetric lens, the deflection angle, α, is given by

$$\alpha = \frac{4G}{c^2} \frac{M(<b)}{b} \tag{6.28}$$

where b is the closest distance between the light ray and the cluster and $M(<b)$ is the projected mass enclosed within this radius. We can express in terms of the geometry of the lens, $b \equiv D_L \theta_I$, where D_L is the distance to the lens and θ_I is the angular separation of the source and lens as seen by the observer.

In the weak lensing case, where $\alpha << \theta_I$, the effect is to distort the background source into a slightly elongated image. The elongation is related to the lensing potential by

$$\begin{pmatrix} e_1 \\ e_2 \end{pmatrix} = \begin{pmatrix} \psi_{11} - \psi_{22} \\ 2\psi_{12} \end{pmatrix} \tag{6.29}$$

where $\psi_{ij} = \frac{\partial^2 \psi}{\partial \theta_i \partial \theta_j}$ and ψ is the lensing potential given by

$$\nabla^2 \psi = \frac{D_L D_{LS}}{D_S} \frac{8\pi G}{c^2} \Sigma$$

where $\Sigma = \int \rho \, dl$ is the projected mass surface density.

These equations can indeed be inverted to map the mass density of the cluster (Kaiser and Squires 1993). For a spherically symmetric cluster, we can relate the distortion to the surface density within a certain radius as

$$\gamma = \frac{\bar{\Sigma}(<b) - \Sigma(b)}{\Sigma_{\text{crit}}} \tag{6.30}$$

where Σ is the mass surface density. While the lensing signal directly measures the gravitating mass of the system, the signal is still subject to confusion by line-of-sight projections, such as the "mass-sheet degeneracy" (Bradac et al. 2004).

In the strong lensing case, the affect on the light path is more extreme and nonlinear. Several different paths through the cluster may result in local stationary points in the path length and thus correspond to images. The brightness of the different images will vary, some being brighter and others fainter. Note that the intrinsic surface brightness of these images is the same; it is their angular extent that differs, and this can give rise to large magnification factors. Although the strong lensing measurements cannot give total cluster mass (since the strong lensing effect is confined to the center of the system), they give a powerful technique for measuring the mass distribution within the Einstein radius. This can, in turn, be used to confirm the mass distribution with the radius probed by X-ray measurements.

4.4 Implications for Cosmology

The presence of dark matter in clusters is clear. All the methods are in broad agreement (see ❯ *Fig. 6-13*), with a much greater mass than can be associated with the galaxies alone, or indeed even with the diffuse intra-cluster plasma. Of course, this does not directly preclude the
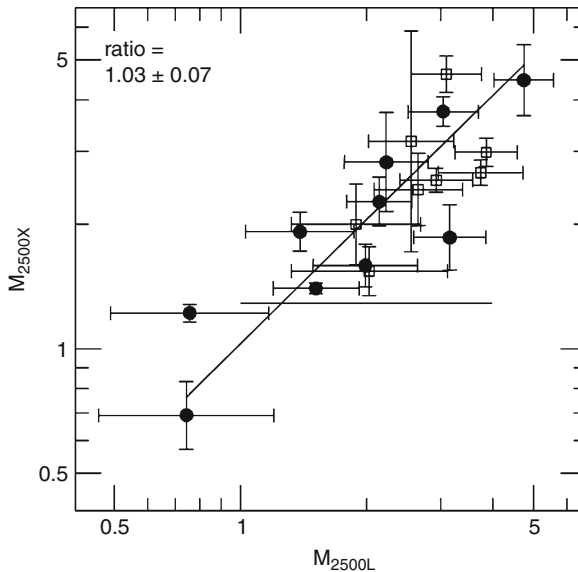
◾ **Fig. 6-13**

Comparison of cluster masses derived from lensing and X-ray studies using the techniques described in the text. The figure is taken from Mahdavi et al. (2008). Masses are computed within a radius of $r_{2,500}$ and are in units of $10^{14}\,M_{\odot}$ (within this radius, the enclosed average density is 2,500 times the critical density). *Solid* and *open symbols* denote clusters with/without central temperature decrements. The *solid line* shows the relation expected if the masses are equal (Image credit: Mahdavi et al. 2008)

dark component being baryonic, but it is hard to imagine any viable way in which the required vast abundance of baryons could be hidden. For example, the necessary mass of dust would greatly exceed the limits on obscuration of background sources. We conclude that most of the mass in cluster is non-baryonic.

Moreover, observations of the microwave background and nucleosynthesis are incompatible with a significant baryonic component. Recent CMB constraints suggest $\Omega_b/\Omega_M = 0.167$ (Komatsu et al. 2011). Allowing for the small (10%) contribution from baryons locked up in stars, this is 13% higher than the observed value in galaxy clusters (Ettori et al. 2009). The remaining factor maybe due to some mass ejected from the halo. This process is clearly seen in galaxy groups, and it is thought that energy injection from AGN is responsible.

Additional cosmological constraints come from the abundance of clusters. They are a sensitive probe of the highest peaks of the primordial density field. To understand how the abundance of clusters can be used as a cosmological constraint, we must understand how clusters are formed.

5   The Formation of Clusters

A full treatment of the evolution of cosmological density perturbation is beyond the scope of this chapter. We provide a very brief outline.

One approach is to consider the evolution of the cosmological density field following the ideas of Press and Schechter (1974). This provides a simple analytical model of the most important features. In the small amplitude regime, the growth of density perturbation is linear and the different Fourier modes can be treated independently.

For a critical density universe, the perturbations, $\delta \equiv \Delta\rho/\rho$, grow as $(1+z)^{-1}$. For a more general cosmology, the growth rate is more complicated, but the principle is the same. However, as the perturbations grow in amplitude, they eventually become large enough that the nonlinear terms in the equations can no longer be ignored. At this point, the growth rate accelerates. When $\delta \sim 1$, the perturbation turns around and decouples from the cosmic expansion. It then rapidly collapses to form a virialized object.

The key idea of the Press–Schechter model is to separate the growth of the perturbation into the linear and nonlinear regimes. In this way, it is possible to count the fraction of space that collapses into objects of a given size. So that the probability that a particle is part of an object of a mass greater than M is given by

$$F \equiv p\big(\delta > \delta_c | R_f(M)\big)\,[\times 2] = \frac{1}{2}\left(1 - \mathrm{erf}\left(\frac{\delta_c}{\sqrt{2}\sigma(R_f,z)}\right)\right)[\times 2] \qquad (6.31)$$

δ_c is the threshold for nonlinear collapse. In the critical density of the universe, this is usually set to 1.68 (to match the behavior expected for a top hot spherical density perturbation). $R_f(M)$ is an appropriate scale corresponding to collapsed objects of mass M. An appropriate choice would be to set this to $(M/(4\pi\rho_0/3))^{1/3}$, where ρ_0 is the average density of the universe. The term $\sigma(R_f,z)$ is the rms amplitude of density fluctuations on scale R_f at redshift z. You should read the left side as giving the probability for collapse when the linear density field has been filtered on scale R_f. The growth on the density fluctuations is encapsulated in the $\sigma(R_f,z)$ term. We can simplify this expression by encapsulating the redshift and mass dependence in $\nu = \frac{\delta_c}{\sigma(R_f,z)}$.

I have included a mysterious term [×2] factor in this expression. If we were to count only regions where the linear field exceeded the density threshold, this term would not appear. However, the formula would then only ever place half the mass of the universe in collapsed objects. Press and Schechter multiplied the expression by 2 so that all the mass is placed in collapsed objects if the threshold is sufficiently low. One argument is that we must account for regions of the universe that are close to over-dense peaks as well as the peaks themselves. As the peak collapses, it pulls in material from the surrounding region. This process does not need to be independent of scale, but the factor of 2 approximation does a remarkably good job. Another way to look at this problem is to examine the trajectories of the density of a point as a function of the filtering scale. In this way, we can avoid undercounting regions (Bond et al. 1991).

In order to derive the mass spectrum of density perturbations, we can differentiate this probability function in order to obtain the mass function of objects with mass M. If we define $f(M)$ as the commoving number of objects of mass M, so that $M f(M)/\rho_0 = |dF/dM|$, we obtain

$$f(M) = \rho_0 M^2 \left| \frac{d \ln \sigma}{d \ln M} \right| \sqrt{\frac{2}{\pi}} \nu \exp\left(-\frac{\nu^2}{2}\right) \tag{6.32}$$

With recent advances in numerical simulations, it is possible to improve on this mass function by more carefully calibrating the terms. A detailed discussion of a better approximation to this mass function, and extension to a wider range of cosmologies can be found in (Reed et al. 2007).

Nevertheless, the simple analytic formula gives remarkable insight into the formation of structures in the universe and the growth of clusters in particular. At the present epoch, the characteristic mass of haloes is ~10^{13} $M_\odot$ and thus clusters represent extreme objects in regions of accelerated structure growth. It is possible to take this picture further and to ask how the growth of a cluster differs from that of an average region of the universe.

Of course, numerical simulations are needed to see the full 3-dimensional picture. It can be seen that clusters are knots formed at the intersection of the filaments. They grow by accreting smaller lumps (such as galaxy groups) as well as more diffuse material that drains in along the filaments. The Press–Schechter model can give insight into the growth statistics, but these can also be determined directly from the numerical models.

An interesting question to ask is, what fraction of a cluster's mass arrives in the form of galaxy groups and what fraction in mass units of individual galaxies or smaller (McGee et al. 2009). A relatively large fraction of galaxies in a cluster have previously been in a group. This raises important issues. The properties of galaxies now in rich clusters might have been largely determined by the environmental interactions at the galaxy group stage.

These theoretical developments allow us to connect together snapshots of galaxies in clusters and groups at different epochs and give us the tools needed to create an empirical history of cluster galaxy formation based on statistical arguments. Our understanding of the growth of clusters also allows us to better trace the growth of the entropy of the intra-cluster medium and to explain the nontrivial scaling of the entropy distribution with cluster mass.

The abundance of clusters is an encouraging cosmological probe. Cluster abundance should vary strongly as a function of the cosmological power spectrum amplitude. Its evolution is a strong function of the background cosmology as illustrated in ❯ *Fig. 6-14*.

The difficulty with these constraints is that cluster masses are not measured directly, but rather use proxy such as X-ray temperature, luminosity, or red galaxy content. Measurements
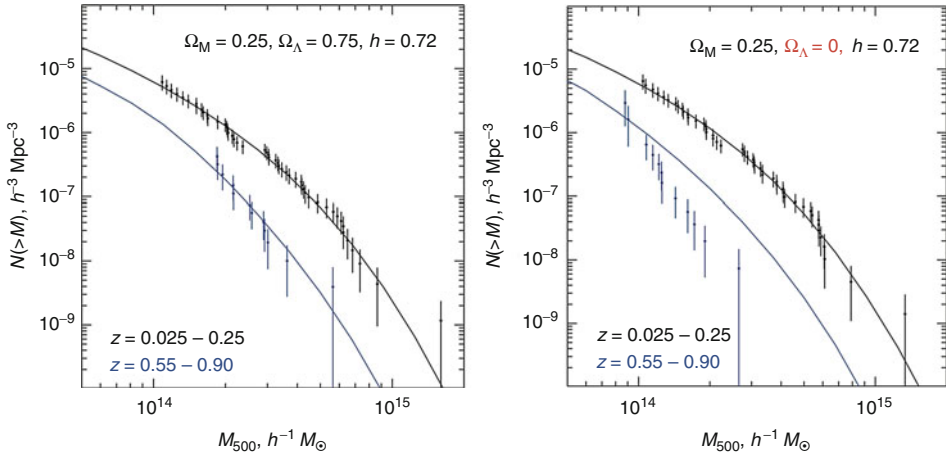
◨ Fig. 6-14

An illustration of the cosmological constraints that may be obtained from measurements of cluster abundance, from Vikhlinin et al. (2009). The black (*blue*) lines distinguish cluster samples at high and low redshift. The two panels compare predictions (*lines*) with observational data. Note that the change of cosmology affects both the observational data (through the luminosity distance and the volume of the survey) and the model prediction (through the growth rates of dark matter haloes) (Image credit: Vikhlinin et al. 2009)

based on the SZ effect may overcome some of the biases, but to make cutting-edge constraints requires control of systematics at better than a 1% level. This may be possible in future surveys, but it is clearly challenging to improve on the tight constraints that come from observations of the cosmic microwave background. Cluster abundance constraints may have a stronger role in constraining (or measuring) non-Gaussian distortion of the power spectrum. These cause the growth rate of clusters to exceed (or lag behind) the rates estimated from the power spectrum and may provide significant insight into the nature of inflation or quintessence (Verde and Matarrese 2009).

6 Summary and the Future

6.1 Summary

This has been a brief introduction to the scientific excitement of galaxy clusters. The picture has changed considerably from the inception of cluster studies based on optical concentrations of galaxies seen in photographic plates. We now realize that the major mass component of the cluster is unseen. It has been revealed through careful dynamical measurements, the high pressure of the intra-cluster plasma in galaxy clusters, and through the distortion of background objects lensed by the gravitational mass of the system. Even amongst the baryonic component, we now realize that the stars in galaxies in the cluster make up a minor contribution. Most of

the baryons in the cluster are in the diffuse, hot plasma that is trapped by the system's gravitational potential. Clusters of galaxies have given us much greater insight into the formation of the universe than just their role as a laboratory for the interactions of galaxies.

In this introduction, we have looked at:

- The optical properties and galaxies. I have emphasized the role clusters play as laboratories for the interactions of galaxies with their environment. "Galaxy ecology" is rapidly gaining momentum and understanding through the comparison of cluster (and group and field) observations over a wide range of redshifts with theoretical models. The study has much to tell us about how galaxies evolve and how star formation in the universe is suppressed.
- X-ray emission and the intra-cluster medium. Clusters of galaxies offer unique insight, because this material cannot be observed in lower mass systems such as the haloes of individual galaxies. Although a "warm–hot intergalactic medium" is needed to reconcile the observed abundance of galaxies and the cosmic baryon density, the WHIM cannot be observed directly, because it is too cold for observation with standard techniques. The intra-cluster medium offers us the best insight into the thermal history of most of the vast majority of baryons in the universe.
- Clusters of galaxies in their cosmological context. Clusters of galaxies also play an important role in cosmology, allowing us to independently confirm the cosmological parameters extracted from analysis of the cosmic microwave background. As the field progresses, the two approaches may take on complementary roles allowing a deep study of the nature of the initial fluctuations that seed galaxy formation in the universe.

Clusters of galaxies still offer a very promising avenue for these research goals and will continue to be the target of observing campaigns for many years to come. It will be exciting to see the new twists that a new generation of astronomers brings to cluster research.

References

Balogh, M. L., Baldry, I. K., Nichol, R., Miller, C., Bower, R., & Glazebrook, K. 2004, ApJ, 615, L101

Balogh, M. L., et al. 2011, MNRAS, 412, 2303

Bamford, S. P., et al. 2009, MNRAS, 393, 1324

Binney, J., & Tabor, G., 1995, MNRAS, 276, 663

Birzan, L., Rafferty, D. A., McNamara, B. R., Wise, M. W., & Nulsen, P. E. J. 2004, ApJ, 607, 800

Bond, J. R., Cole, S., Efstathiou, G., & Kaiser, N. 1991, ApJ, 379, 440

Bower, R. G., Benson, A. J., Malbon, R., Helly, J. C., Frenk, C. S., Baugh, C. M., Cole, S., & Lacey, C. G. 2006, MNRAS, 370, 645

Boylan-Kolchin, M., Ma, C.-P., & Quataert, E. 2008, MNRAS, 383, 93

Bradac, M., Lombardi, M., & Schneider, P. 2004, A&A, 424, 13

Brinchmann, J., Charlot, S., White, S. D. M., Tremonti, C., Kauffmann, G., Heckman, T., & Brinkmann, J. 2004, MNRAS, 351, 1151

Butcher, H., & Oemler, A., Jr. 1984, ApJ, 285, 426

Chandrasekhar, S. 1943, ApJ, 97, 255

Churazov, E., Brüggen, M., Kaiser, C. R., Böhringer, H., & Forman, W., 2001, ApJ, 554, 261

Couch, W. J., & Sharples, R. M. 1987, MNRAS, 229, 423

Covington, M., Dekel, A., Cox, T. J., Jonsson, P., & Primack, J. R. 2008, MNRAS, 384, 94

De Lucia, G., et al. 2004, ApJ, 610, L77

Dekel, A., & Birnboim, Y. 2006, MNRAS, 368, 2

Dressler, A. 1980, ApJ, 236, 351

Dressler, A., et al. 1997, ApJ, 490, 577

Edge, A. C. 2001, MNRAS, 328, 762

Ettori, S., Morandi, A., Tozzi, P., Balestra, I., Borgani, S., Rosati, P., Lovisari, L., & Terenziani, F. 2009, A&A, 501, 61

Fabian, A. C. 1994, ARA&A, 32, 277

Fabian, A. C., Sanders, J. S., Taylor, G. B., Allen, S. W., Crawford, C. S., Johnstone, R. M., & Iwasawa, K. 2006, MNRAS, 366, 417

Geach, J. E., Smail, I., Moran, S. M., Treu, T., & Ellis, R. S. 2009, ApJ, 691, 783

Gladders, M. D., & Yee, H. K. C. 2000, AJ, 120, 2148

Gonzalez, A. H., Zabludoff, A. I., & Zaritsky, D. 2005, ApJ, 618, 195

Gunn, J. E., & Gott, J. R., III 1972, ApJ, 176, 1

Haines, C. P., et al. 2009, ApJ, 704, 126

Hammer, D., et al. 2010, ApJS, 191, 143

Holden, B. P., et al. 2005, ApJ, 620, L83

Jorgensen, I., Franx, M., & Kjaergaard, P. 1996, MNRAS, 280, 167

Kaiser, N., & Squires, G. 1993, ApJ, 404, 441

Kennicutt, R. C., Jr. 1998, ARA&A, 36, 189

Komatsu, E., et al. 2011, ApJS, 192, 18

Leccardi, A., & Molendi, S., 2008, A&A, 487, 461

Lintott, C.J., Schawinski, K., Slosar, A., Land, K., Bamford, S., Thomas, D., Raddick, M.J., Nichol, R.C., Szalay, A., Andreescu, D., Murray, P., & Vandenberg, J. 2008, Galaxy Zoo: morphologies derived from visual inspection of galaxies from the Sloan Digital Sky Survey. *Monthly Notices of the Royal Astronomical Society*, 389, 1179–1189.

Mahdavi, A., Hoekstra, H., Babul, A., & Henry, J. P. 2008, MNRAS, 384, 1567

Maier, C., et al. 2009, ApJ, 694, 1099

McCarthy, I. G., Frenk, C. S., Font, A. S., Lacey, C. G., Bower, R. G., Mitchell, N. L., Balogh, M. L., & Theuns, T. 2008, MNRAS, 383, 593

McCarthy, I. G., Schaye, J., Bower, R. G., Ponman, T. J., Booth, C. M., Vecchia, C. D., & Springel, V. 2011, MNRAS, 412, 1965

McGee, S. L., & Balogh, M. L. 2010, MNRAS, 403, L79

McGee, S. L., Balogh, M. L., Bower, R. G., Font, A. S., & McCarthy, I. G., 2009, MNRAS, 400, 937

McNamara, B. R., Nulsen, P. E. J., Wise, M. W., Rafferty, D. A., Carilli, C., Sarazin, C. L., & Blanton, E. L. 2005, Nature, 433, 45

Moore, B., Katz, N., Lake, G., Dressler, A., & Oemler, A. 1996, Nature, 379, 613

Nelan, J. E., Smith, R. J., Hudson, M. J., Wegner, G. A., Lucey, J. R., Moore, S. A. W., Quinney, S. J., & Suntzeff, N. B. 2005, ApJ, 632, 137

Peacock, J. A. 1999, in Cosmological Physics, ed. J. A. Peacock (Cambridge, UK: Cambridge University Press), 704. ISBN 052141072X

Peng, Y.-j., et al. 2010, ApJ, 721, 193

Peres, C. B., Fabian, A. C., Edge, A. C., Allen, S. W., Johnstone, R. M., & White, D. A. 1998, MNRAS, 298, 416

Peterson, J. R., Kahn, S. M., Paerels, F. B. S., Kaastra, J. S., Tamura, T., Bleeker, J. A. M., Ferrigno, C., & Jernigan, J. G. 2003, ApJ, 590, 207

Ponman, T. J., Cannon, D. B., & Navarro, J. F. 1999, Nature, 397, 135

Pratt, G. W., et al. 2010, A&A, 511, A85

Press, W. H., & Schechter, P. 1974, ApJ, 187, 425

Quilis, V., Bower, R. G., & Balogh, M. L. 2001, MNRAS, 328, 1091

Reed, D. S., Bower, R., Frenk, C. S., Jenkins, A., & Theuns, T. 2007, MNRAS, 374, 2

Richstone, D. O. 1975, ApJ, 200, 535

Saintonge, A., Tran, K.-V. H., & Holden, B. P. 2008, ApJ, 685, L113

Sanderson, A. J. R., Ponman, T. J., & O'Sullivan, E. 2006, MNRAS, 372, 1496

Sarazin, C. L. 1988, X-ray Emissions from Clusters of Galaxies, Cambridge Astrophysics Series (Cambridge: Cambridge University Press)

Simard, L., et al. 2002, ApJS, 142, 1

Stott, J. P., Smail, I., Edge, A. C., Ebeling, H., Smith, G. P., Kneib, J.-P., & Pimbblet, K. A. 2007, ApJ, 661, 95

Sutherland, R. S., & Dopita, M. A. 1995, ApJ, 439, 381

Verde, L., & Matarrese, S. 2009, ApJ, 706, L91

Vikhlinin, A., Kravtsov, A., Forman, W., Jones, C., Markevitch, M., Murray, S. S., & Van Speybroeck, L. 2006, ApJ, 640, 691

Vikhlinin, A., et al. 2009, ApJ, 692, 1060

White, S. D. M., & Frenk, C. S. 1991, ApJ, 379, 52

Wiersma, R. P. C., Schaye, J., & Smith, B. D. 2009, MNRAS, 393, 99

Worthey, G. 1994, ApJS, 95, 107